Room Geometries with non-classical Reverberation Times

Asta Rønning Fjærli

Problem Description

Room Geometries with non-classical Reverberation Times

Classical diffuse field theory is a simplified theory in room acoustics, which leads to Sabine's and Eyring's predictions of reverberation time. For a room with highly scattering surfaces, Sabine's and Eyring's estimates of reverberation time will be closely related to the real conditions. In rooms with a low degree of scattering and an uneven distribution of absorption, however, Sabine's and Eyring's formulae often underestimates the reverberation time. In this case, an increase of the scattering will always lead to a shorter reverberation time,

In this project, there will be examined which type of rooms that can give a shorter reverberation time than Sabine's and Eyring's predictions. Types of rooms suggested by Stephenson, and rooms with the tendency of a focus effect, can be studied. Computer simulations based on geometrical acoustics can be used, together with other existing reverberation time formulae than the classical formulae by Sabine and Eyring.

Romgeometrier med ikke-klassiske etterklangstider

Klassisk diffusfeltsteori er en forenklet teori innen romakustikk som leder til Sabines og Eyrings prediksjoner av etterklangstid. Hvis et rom har høy grad av spredning vil Sabines og Eyrings etterklangsestimat meget ofte være nært de virkelige forholdene. I rom med lav grad av spredning og ujevn fordeling av absorpsjon er det derimot ofte slik at Sabines og Eyrings likninger underestimerer etterklangstiden. I slike fall vil en økning av spredningen i rommet alltid lede til kortere etterklangstid.

I dette prosjektet skal det undersøkes hvilke typer rom som kan gi kortere etterklangstid enn Sabines og Eyrings prediksjoner. Typer av rom som er foreslått av Stephenson, og rom med tendenser til fokuseffekter, kan studeres. Datasimuleringer basert på geometrisk akustikk kan brukes, sammen med andre eksisterende etterklangsformler enn de klassiske av Sabine og Eyring.

Abstract

In this Master's thesis, it has been examined whether it is possible to find rooms of such a geometry that the reverberation time becomes shorter than the predicted value of Sabine and Eyring. This was investigated using the computer program CATT-Acoustic, which is based on geometrical acoustics. The geometries of the rooms were polyhedral approximations of a dome; respectively a decahedron, a nonahedron and a hexahedron, the latter of which also representing a "shoe-box shaped" room with inclined walls.

The results of the simulations show a clear tendency of a lowered reverberation time compared to the two classical formulae. For a large floor absorber and a scattering coefficient of $s > 10 - 20\%$, the three polyhedral approximations all give a ratio of $\frac{T_{30}}{T_{Eyring}} < 1$. However, it is not possible to conclude that a focusing effect, like what one can find in a dome, is the reason for this ratio. The lack of support for such a focusing effect follows follows from the dependency on the number of surfaces in the polyhedral approximation. The decahedron is a closer approximation to a dome than the hexahedron, but the three polyhedra give approximately the same ratio of simulated and predicted reverberation times. The simulated values were also compared to what can be found using Millington-Sette's reverberation formula and Kuttruff's formula for the absorption coefficient. These formulae both gave significantly lower values of the reverberation time than the simulations. Therefore, the alternative formulae do not seem to be any better alternatives than the classical Eyring's formula. Detailed calculation using ray tracing should anyway be used for cases like those tested here, with uneven distributions of absorption.

Sammendrag

Det har i denne masteroppgaven blitt undersøkt om det finnes rom av en slik geometri at etterklangstiden blir kortere enn de beregnede verdiene fra Sabines og Eyrings likninger. Dette ble undersøkt ved å gjennomføre simuleringer i CATT-Acoustic, som er en programvare basert på geometrisk akustikk. Geometriene implemetert i CATT-Acoustic var polyhedratilnærminger av et kuppelrom; henholdsvis et dekahedron, et nonahedron og et hexahedron. Sistnevnte representerer et "skoeskerom" med tiltede vegger.

Resultatene fra simuleringene viser en tendens til en redusert etterklangstid sammenliknet med de to klassiske formlene. For en stor gulvabsorbent og en spredningskoeffisient på $s > 10-20\%$ gir de tre polyhedratilnærmingene en ratio på $\frac{T_{30}}{T_{Eyring}} < 1$. Det er imidlertid ikke mulig å konkludere med at en fokuseffekt, som den man finner i en kuppel, er grunnen til dette forholdet. Årsaken til at man ikke kan påstå at en fokuseffekt er forklaringen følger av sammenhengen med antall flater i polyhedratilnærmingen. Et dekahedron er en bedre tilnærming til en kuppel enn et heksahedron, men de tre polyhedraene gir likevel tilnærmet likt forhold mellom simulert og beregnet etterklangstid. De simulerte verdiene ble også sammenlignet med etterklangstidene man får ved å bruke Millington-Settes etterklangsformel og Kuttruffs formel for absorpsjonskoeffisienten. Disse formlene ga begge betraktelig lavere verdier for etterklangstiden enn simuleringene gjorde. De alternative formlene for etterklangstid ser derfor ikke ut til å være bedre alternativer enn den klassiske Eyrings formel. Detaljerte beregninger med bruk av ray tracing må uansett benyttes for tilfeller som de som er studert i denne masteroppgaven, der absorpsjonen er ujevnt fordelt.

Preface

This Master's thesis is the response to the problem description *Room geometries with non-classical reverberation times* suggested by Professor Peter Svensson and Senior Acoustic Consultant Magne Skålevik. The subject was given by the Department of Electronics and Telecommunications spring 2015, but the report is presented as the result of the course TFY4900 - Physics, Master's thesis. This course is mandatory in the 10th semester of the master program of applied physics.

Peter Svensson and Magne Skålevik have been the supervisors on this thesis, with Jon Andreas Støvneng as the contact at the department of physics. I would like to thank Peter and Magne for valuable guidance and interesting discussions on my work with this report, and Jon Andreas for helping with the practical issues by performing my Master's thesis for the Department of Electronics and Telecommunications. Finally I would like to thank Anne Birgitte Rønning and Erik Fjærli for correcting my typos and mistakes in the manuscript and give constructive advices in the writing process.

Asta Rønning Fjærli
Trondheim, June 25, 2015

Contents

List of Figures

List of Tables

Abbreviations and symbols

- ISM - Image Source Method

- RT - Ray Tracing

- mfp - Mean free path

- CI - Confidence interval

- IR - Impulse response

- CATT - CATT-Acoustic

- TUCT - The Universal Cone Tracer

- T - Reverberation time

- V - Volume

- S - Surface area

- s - Scattering coefficient

- α - Absorption coefficient

- ρ - Reflection coefficient

- θ - Wall inclination angle

1 Introduction

1.1 Motivation

In the work of an acoustic consultant, it passes up to several years from the planning of a new project till it is finished and verifying measurements can be performed. Basing following projects on the same idea may therefore have unsure outcomes. Consequently, it is of vital interest for the consultant sector to get more control on the prediction phase of a project to prevent surprises on the finish line.

One solution to this problem is to perform scale model measurements before starting the construction of a full scale room or building. However, this is often an expensive solution. In addition, there are limitations in the usage of scale model measurements as well, both in the choice of materials that correspond to the full scale materials and in the treatment of air absorption. There exist several acoustic simulation programs based on geometrical acoustic methods like ray tracing (RT) and the image source method (ISM), that can predict the outcome of a new idea. The use of such programs is less expensive and more time efficient alternatives compared to scale model measurements. Examples of acoustic simulation programs are programs are ODEON and CATT-Acoustic, and CATT-Acoustic is the software that will be used in this Master's thesis.

As will be presented in section 1.2, the author has earlier investigated the effect of a new type of ceiling diffusers first used by Arau Acoustica [1], using a scale model. The measurements of Arau Acoustica showed a prolonged reverberation time with the ceiling diffuser present compared

to initial measurements, which is a surprising result considering existing reverberation formulae which only give a relationship between the reverberation time, the room volume and the average absorption in the room.

The following situation may be regarded as the opposite of what was done in the Theatre of Liceu:

An existing room has a ceiling diffuser, and the interest of the acoustician is to increase the volume of the room, assuming a prolonged reverberation time based on Sabine's and Eyring's equations. Therefore, the diffuser is removed, and one expects to get a longer value for the reverberation time. However, in the case of the rehearsal room in Liceu, the reverberation time without the diffuser is shorter, even if the room volume is larger without the diffuser.

The result of a shortened reverberation time with a larger room volume is surprising compared to the classical predictions. This is the motivation to study the problem further, and to try to find other room geometries that give shorter values than Sabine's and Eyring's formulae predict. It is also interesting to investigate whether there exist other reverberation formulae that give better values for such room geometries than the classical formulae of Sabine and Eyring.

A focusing room shape, like a dome with a reflecting ceiling and an absorbing ground flate, could make a floor absorber more effective, and thus lead to a shorter reverberation time than T_{Sabine} [2]. An opposite of this situation is the so-called *Hard Case* [3], [4]. The *Hard Case* is a cuboid room represented by hard walls and a hard floor, with a ceiling absorber as the only absorbing element. In this case, the reverberation time becomes longer than Sabine's and Eyring's predictions. In addition, due to an almost two-dimentional sound field at high frequecies, flutter echo may occur.

1.2 Previous work

In the specialization project carried out by the same author the autumn semester 2014, the findings of Arau-Puchade's work in the Rehearsal Room of the Great Theatre of Liceu [1] were examined in a scale model with a scale factor of 1 : 8. Arau-Puchades installed a ceiling diffuser in this rehersal room, consisting of a regular metal grid with vertical polycarbonate plates forming a labyrinth structure. The scale model diffuser is shown in Figure 1.1 Arau-Puchades' acoustic measurements before and after the diffuser was installed show a significantly shortening reverberation time, considering both the T_{30} and the EDT.
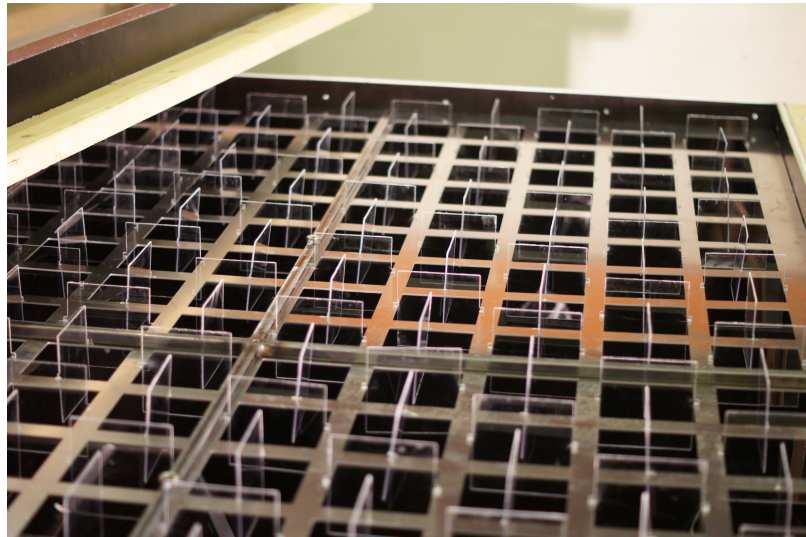
Figure 1.1: The scale model diffuser used in the specialization project autumn 2014.

The reverberation time measurements in the scale model did not follow the same pattern as the full scale measurements of Arau, but studies of the curvature C showed that the ceiling diffuser made a significant impact on the diffusivity of the room. The results of this specialization project lead to further questions about the validity of the classical reverberation time formulae and the treatment of non-diffuse sound fields.

1.3 Report structure

A theoretical background for the simulations is first presented in chapter 2, together with a study of the classical diffuse field theory. In chapter 3, the experiments in CATT-Acoustic are explained. The result of these simulations is presented in chapter 4 and further discussed in chapter 5. The concluding remarks follow in chapter 6.

There are three appendices to this report. Appendix A contains two tables; a table of the corners in the hexahedron approximation given different inclination angles and a table for the absorption coefficient given different materials. The mean values of the simulations are plotted in appendix B. Finally, the Matlab code used to find the corners of a polygon follows in appendix C together with the Matlab code generated to read the TUCT-text files from CATT-Acoustic.

2 Theory

This chapter will introduce some of the parameters that will be analyzed in this thesis, primarily concerning reverberation time and characteristics of a diffuse sound field. There are different approaches to a theoretical value of the reverberation time, which will be presented together with their historical background. The importance of a diffuse sound field for these formulae to be valid is also introduced. Geometrical variations in room design and their influence of the reverberation time will then be presented, and thereafter the theory underlying the simulation software CATT-Acoustic and other room acoustic computer models.

2.1 Reverberation time

When it comes to room acoustics the reverberation time is usually judged to be the most important parameter. The reverberation time is often represented by T_{30} and can be measured in a room using the impulse response, it can be predicted by reverberation formulae or it can be predicted using geometrical acoustic methods. The reverberation time is a global parameter, which means that the measure is independent of the positions in a room [5]. By contrast, acoustical parameters such as sound strength (G), early decay time (EDT), clarity (C_{80}), lateral energy fraction (LEF) and the late sound level (G_{late}) are local acoustical parameters and dependent on the location of the listener.

ISO 3382-2 defines the reverberation time as the *duration required for the space-averaged sound energy density in an enclosure to decrease by 60 dB*

after the source emission has stopped [6]. In this definition, the sound decay is regarded as a stepwise decrease, which means that the sound persists and does not disappear immediately after the sound source is cut off.

Representing the reverberation time by the measure of T_{30} implies that the first 30 dB decrease, from -5 dB to -35 dB, is used for a linear regression of the total 60 dB decrease. The same concept applies for the T_{20}, which concerns the decrease from -5 dB to -25 dB as a base for the regression. The reason for the use of T_{20} and T_{30}, instead of using the full 60 dB decrease, is that the difference between the background noise and the sound signal is usually smaller than 60 dB. The early part of the sound decay is also usually the most interesting part [7]. Figure 2.1 represents the Schroeder curve for the simulations of the decahedron room in CATT-Acoustic, and gives the sound decay in dB as a function of the elapsed time. A Schroeder curve shows the backwards integration of the squared impulse response [8].
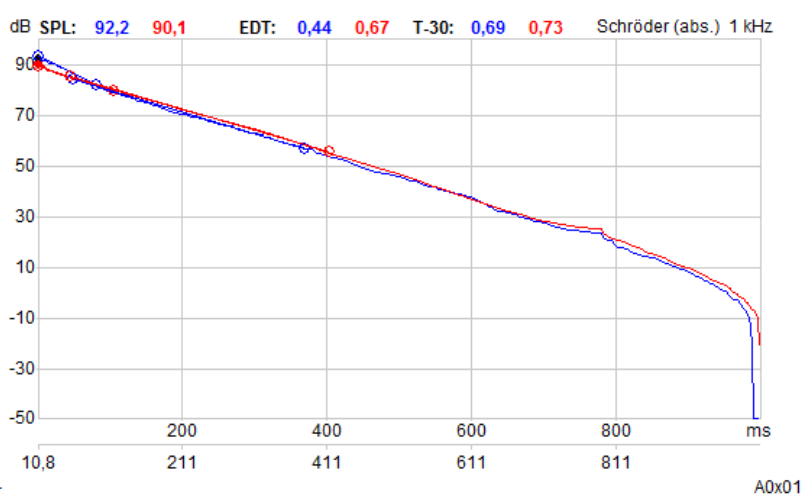
Figure 2.1: The Schroeder curve, obtained in CATT-Acoustic for one of the rooms studied in this thesis.

The optimal reverberation time of a room is dependent on both the application for the room, the volume of the room and on the frequency spectrum. A longer reverberation time is recommended at low frequencies, while mid-frequencies can have a longer reverberation time [9, p. 86]. To obtain a room with good articulation for speech, for instance, a short reverberation time is necessary, while acoustic music requires a

longer reverberation time. Church music is an extreme and requires a reverberation time of several seconds. To obtain the optimal reverberation time, it is also necessary to consider the size of the room. For a larger room volume longer reverberation time would be preferable.

The optimal reverberation times for different sound sources are presented in Table 2.1 [10, p. 504], [11, p. 313]. Beranek's value for symphony orchestras is based on best ratings of 40 concert halls presented in *Concert halls and opera houses* and is valid for mid-frequencies. The lowest rated halls in Beranek's study had in comparison a reverberation time in the range of $T = 1.5 - 1.8$ s.

Table 2.1: Optimal reverberation times for different sound sources.

Sound source	Optimal reverberation time [s]
Symphonical music (Beranek)	1.8 - 2.0
Symphony orchestra (Gade)	2.0 - 2.4
Chamber music (Gade)	1.5
Opera (Gade)	1.4 - 1.8
Rythmic music (Gade)	0.8 - 1.5

2.1.1   The absorption coefficient

An important parameter that influences the reverberation time in a room is the absorption coefficient and the average absorption. For a room with total surface area S and segmental absorption areas S_i with corresponding absorption coefficients α_i, the average absorption is given by

$$\bar{\alpha} = \frac{1}{S} \sum_i (S_i \alpha_i) \tag{2.1}$$

This equation does not tell how the absorption is distributed in a room. The effect of uneven distribution of absorption will be introduced in section 2.1.2 and discussed further in section 5.7.

2.1.2 Diffuse sound fields

The length of a sound decay is dependent on the structure of the sound field in a room. The classical formulae, like the formulae of Sabine and Eyring, assumes a diffuse sound field. In a diffuse sound field, all directions of sound propagation are equally likely, and the sound pressure level is independent of the location [12]. The measured reverberation time will therefore be constant for all positions of the sound source and the receivers in a room. In real life, however, one will never achieve a perfect diffuse sound field.

For a diffuse sound field, theory predicts a pure exponential sound decay [11, p. 307-308]. For such a decay the dB-curve is linear. In this situation, the reverberation time T is independent of the evaluated decay range, giving $T_{30} = T_{20} = T_{60}$. The intensity of a sound field is given by $I(\phi, \nu)$ where ϕ and ν give the directions of the distribution. The energy density is then given by $dw = \frac{I(\phi,\nu)}{c} d\Omega$ [13, p. 129], where c is the speed of sound and $d\Omega$ represents a very small solid angle in a collection of nearly parallell sound rays. For a 3-dimentional diffuse sound field, this intensity is constant, which gives total sound energy density in all directions $w = \frac{4\pi I}{c}$.

To obtain a diffuse sound field, it is claimed that absorption is evenly distributed over all surfaces of the room and that one has scattering surfaces. The amount of diffusivity in a room will also influence the effectiveness of the absorption [14]. The assumption of a diffuse field is valid for frequencies above the Schroeder frequency, f_s [12]. The Schroeder frequency is given by

$$f_s = 2000\sqrt{\frac{T}{V}}, \tag{2.2}$$

where T represents the reverberation time and V is the volume of the room. For frequencies beneath the f_s, the sound field cannot be considered to be diffuse. This limit claims that the volume of a room has to be large compared to the acoustic wavelengths [15]. To obtain a lower Schroeder frequency one must either decrease the reverberation time, for instance by increasing the absorption coefficient, or increase the room volume.

Examples of rooms that cannot be classified as diffuse are rooms with a majority of the absorption concentrated on one side, for instance the so-called *Hard Case*, and coupled rooms. An example of the absorbing surface is acoustic ceiling tiles, or it can be the audience giving an absorbing floor. Odd-shaped rooms, for instance a long corridor measuring $A \cdot B \cdot C$ with $C \gg A$ and $C \gg B$, will also be classified as non-diffuse.

For a unit area of 1 m^2 and a unit time of 1 s, the acoustic intensity in the diffuse sound field with energy density dw is given by [9, p. 66]:

$$I = \frac{c}{4}E. \tag{2.3}$$

This can be compared to the acoustic intensity of a plane wave at normal incidence of the wall, $I = cE$, being four times the acoustic intensity in a diffuse sound field.

2.1.3 The mean free path

The mean free path (mfp), l_m, is the mean distance between two sound reflections. The mfp represents the average distance travelled by the sound waves of sound speed c after a time t from the first wave progagation,

$$l_m n = ct, \tag{2.4}$$

where n is the number of reflections [9, 68].

For a 3-dimentional room of volume V with a diffuse sound field and surface area S, the mean free path is given by [15]

$$l_m = \frac{4V}{S}. \tag{2.5}$$

Equation 2.5 for the mean free path is only valid for strongly diffuse sound fields. Such fields are an assumption for Sabine's and Eyring's formulae.

2.1.4 Sabine's formula

The first scientist to introduce the reverberation time T [s] as a measure of the reverberation in a room was W. C. Sabine. In *The American Arcitect* [16, p. ix], 1900, Sabine presented a relationship between the room volume V, the equivalent absorption area A and the reverberation time T as

$$T \propto \frac{V}{A}. \tag{2.6}$$

In other words, he found the reverberation time to be proportional to the volume of the room and inverse proportional to the absorption, by a proportionality factor K.

Sabine's formula is based on experimental work, but it can also be deduced theoretically. From measurements in the lobby of the Fogg museum and the Jefferson physical laboratory, he found an average proportionality factor of 0.164 [16, p. 50], using SI-units. This value is later found to be 0.161 for sound speed $c = 343$ m/s, giving Sabine's formula

$$T = \frac{0.161V}{A}, \tag{2.7}$$

where A gives the equivalent absorption area $A = S\bar{\alpha} = \sum_i S_i \alpha_i$ for i surfaces. A is given in metric sabin. This formula is neglecting the influence of air absorption. The air absorption is represented by a term presented in section 2.1.7

Sabine's formula follows from the relationship of the total energy in a room with surface area S and energy density E [9, p. 66],

$$V\frac{dE}{dt} = W - \frac{cES\bar{\alpha}}{4}. \tag{2.8}$$

Substituting $S \cdot \bar{\alpha} = A$, and name the initial values $E = 0$ and $t = 0$, gives

$$E = \frac{4W}{cA}[1 - e^{-(cA/4V)/t}]. \tag{2.9}$$

When time passes, $t \to \infty$, the energy will approach the steady-state value $E_0 = \frac{4W}{cA}$. This leads to the total energy reduction in the room,

$$E = E_0 e^{-(cA/4V)/t}, \qquad (2.10)$$

which gives the decay rate $D = 10log(e^{cA/4V})$ with a unit dB per second.

The definition of the reverberation time was presented in section 2.1, and the reverberation time T can be expressed mathematically as

$$T = \frac{60}{D} = \frac{60}{10 \cdot log(e^{cA/4V})} = \frac{6 \cdot 4V}{cA \cdot log(e)} = const \cdot \frac{V}{A}. \qquad (2.11)$$

The constant in equation 2.11 is given by

$$K = \frac{24}{c \cdot log(e)} \approx 55.3 \cdot \frac{1}{c}. \qquad (2.12)$$

For room temperature, $T = 20 \, ^o$, the speed of sound equals $c = 343$ m/s, and the constant, using SI-units, approximates $K = 0.161$. This gives Sabine's formula as presented in equation 2.7.

2.1.5 Eyring's formula

The experimental rooms in which Sabine used to find the reverberation formula all had a reverberation time $T \, \epsilon \, [1.5 - 4]$ s [17]. Such rooms can be classified as "live" rooms. For "dead" rooms, when the average absorption approaches $T = 1$, a weakness of the Sabine's formula appears. For $\bar{\alpha} \to 1$, $A = S\bar{\alpha} \approx S$ and the reverberation time $T_{Sabine} \approx \frac{0.161V}{S}$. This is the opposite of what one would assume for a highly absorbent room where the sound is rapidly damped. This was the motivation of C. F. Eyring, who in 1929 released his alternative to a reverberation formula.

Eyring's formula is based on the assumption that a sound field is composed of plane sound waves. Such waves will lose energy each time they hit an absorbing surface. The fraction of energy lost due to absorption is equal

to $(1 - \bar{\alpha})$ where $\bar{\alpha}$ is the absorption coefficient of the surface. For a given number n of surface reflections, the energy loss is then given by [9, p. 68]

$$E = E_0 \cdot (1 - \bar{\alpha})^n = E_0 \cdot e^{n \cdot ln(1-\bar{\alpha})}, \tag{2.13}$$

With the mean free path expressed as in section 2.1.2, the sound waves will travel an average distance of $l_m n = ct$ where t is the time after the first wave propagation. Substituting $n = ct/l_m$ in equation 2.13, the energy density yields

$$E = E_0 \cdot e^{\frac{c}{l_m} \cdot ln(1-\bar{\alpha})t} \tag{2.14}$$

after a time t.

A 60 dB decrease in sound level means that the energy has dropped to $E = 10^{-6} \cdot E_0$, giving

$$e^{\frac{c}{l_m} \cdot ln(1-\bar{\alpha})T} = 10^{-6}, \tag{2.15}$$

or

$$\frac{c}{l_m} \cdot ln(1 - \bar{\alpha})T = -6 \cdot ln(10). \tag{2.16}$$

The formula of Eyring then follows from the mean free path in a diffuse sound field, given in equation 2.5, and the sound speed for a temperature of 20° C, $c = 343$ m/s. The reverberation formula is presented as

$$T = \frac{6ln(10) \cdot 4V}{-cSln(1 - \bar{\alpha})} = \frac{0.161V}{-Sln(1 - \bar{\alpha})}. \tag{2.17}$$

For rooms with a high average absorption, Eyring's theory gives a better value for the reverberation time than the theory of Sabine. With $\bar{\alpha} \to 1$, which is the situation of the anechoic room, Sabine's formula will give a value of $T \to \frac{0.161V}{S}$, while Eyring's formula, as expected for this room, gives $T \to 0$. For a low average absorption, $\bar{\alpha} < 0.3$ [2], however, the energy

density as viewed from a surface element can be considered continuous since a majority of the incoming energy is reflected. As a result, $\frac{-1}{ln(1-\bar{\alpha})} \approx \frac{1}{\bar{\alpha}}$ and $T_{Eyring} \approx T_{Sabine}$.

2.1.6 Millington-Sette's formula

Millington (1932) [18] and Sette (1933) [19] investigated an alternative to Eyring's reverberation formula. The average absorption coefficient introduced in section 2.1.1 and used in the formulae of Sabine and Eyring regards the number N of collisions by a sound particle as a statistical value, with expectation value $N_i = NS_i/S$ [13, p. 141].

By use of the exact value of N rather than the statistical value, the energy distribution will still follow the exponential equation given in 2.10, but with an average absorption given by

$$\bar{\alpha}' = -\frac{1}{S} \sum_i S_i ln(1 - \alpha_i). \tag{2.18}$$

With this absorption coefficient, Millington and Sette predict a shorter reverberation time than Eyring's formula. This reverberation time is given by

$$T_{Millington-Sette} = 0.161 \frac{V}{S\bar{\alpha}'}. \tag{2.19}$$

The difference between the formula of Millington-Sette and the formulae of Sabine and Eyring lies in the treatment of the absorption coefficient. In equation 2.18, one considers the average of the terms $-S_i ln(1 - \alpha_i)$ and sums over these values rather than taking the logarithm of the average absorption as Eyring did.

Millington-Sette's formula is not meant as a general formula for the reverberation time, but as a supplement to Eyring's formula for the special cases of which Eyring's prediction is not valid [19]. While Eyring's formula gives the expected value of $T \to 0$ for an average absorption of $\bar{\alpha} = 1$, the Millington-Sette's absorption coefficient will develop as $\bar{\alpha}' \to \infty$ for

$\alpha_i = 1$, independent of the size of the corresponding S_i. The resulting reverberation time will then be zero, which is a counterintuitive result.

2.1.7 The influence of air absorption

The three equations 2.7, 2.17 and 2.19, are all presented on the easiest form, neglecting the air absorption. This assumption is only valid for low frequencies. If one includes the air absorbtion, another absorption term $A = 4mV$ is included in the reverberation formula. Here, m is a frequency dependent absorption coefficient for the air absorption [20, p. 338],

$$m = 5.5 \cdot 10^{-4} \left(\frac{50}{h}\right) \left(\frac{f}{1000}\right)^{1.7}, \qquad (2.20)$$

giving

$$A_{air} = 4 \cdot \frac{0.275 f^{1.7}}{h} V. \qquad (2.21)$$

In this equation, h is the percentage of humidity in the room and f is the frequency.

Including the air absorption, Sabine's, Eyring's and Millington-Sette's equations are modified and given in equations 2.22, 2.23 and 2.24:

$$T_{60,Sabine} = \frac{0.161 \cdot V}{A + 4mV}, \qquad (2.22)$$

$$T_{60,Eyring} = \frac{0.161 \cdot V}{-Sln(1 - \bar{\alpha}) + 4mV}, \qquad (2.23)$$

$$T_{60,Millington-Sette} = \frac{0.161 \cdot V}{S\bar{\alpha}' + 4mV}. \qquad (2.24)$$

By concidering the air absorption term in the equations above, it is clear that the air absorption will mostly influence the reverberation in rooms of a large volume and for high frequencies. In scale model measurements, the

frequency f, the volume V and scale factor σ are related by $f_{scale} = f_{real} \cdot \sigma$ and $V_{scale} = V_{real} \cdot \sigma^3$. The treatment of the air absorption is therefore an important issue in scale model measurements.

2.1.8 Fitzroy's formula

In the study of rooms with uneven absorption distribution, Fitzroy [21] found that Sabine's and Eyring's predictions are too low in many cases. Therefore, he came up with a different approach to a theoretical reverberation formula, valid for shoe-box shaped rooms with hard walls and floor and a highly absorbing ceiling. Fitzroy's formula follows from equation 2.25.

$$T_{tot} = \left(\frac{x}{S}\right)\left[\frac{0.161V}{-Slog(1-\alpha_x)}\right] + \left(\frac{y}{S}\right)\left[\frac{0.161V}{-Slog(1-\alpha_y)}\right] + \left(\frac{z}{S}\right)\left[\frac{0.161V}{-Slog(1-\alpha_z)}\right].$$
$$(2.25)$$

In this formula, x represents the total area of the side walls, y is the total area of the ceiling and floor and z is the total area of the end wall. For the surfaces $i = x, y, z$, α_i is the average absorption of the respective area. S is the total surface area and V is the volume of the room.

2.1.9 Kuttruff's absorption formula

In the fourth edition of *Room Acoustics* [22, p. 141], H. Kuttruff introduces an alternative formula for the absorption distribution in a room, which can be used together with Eyring's equation to get a more accurate prediction of the reverberation time for rooms in which the sound field is not diffuse. Kuttruff claims that each boundary gives diffuse reflections, and takes the average number of reflections by a sound particle into account.

Using this absorption formula, one expects a more correct value of absorption for cases where the effective absorption is greater than the absorption coefficient predicted in Eyring's formula. These are cases where

the real reverberation time will be shorter than the one predicted by Eyring.

Kuttruff's absorption formula assume the irradiation strength [22, p. 139] to be constant, and yields

$$a* \approx a_{Eyring} + \frac{\sum \rho_n (\rho_n - \bar{\rho}) S_n^2}{(\bar{\rho} S)^2}.$$
(2.26)

In this formula, ρ is the average reflection, $\rho = 1 - \alpha$. A totally absorbing surface is then characterized by $\rho = 0$. Kuttruff claims that this correction applies well for situations where only one surface has absorption in which differs from the $n - 1$ remaining surfaces, for instance the case of a room with hard walls and a floor occupied by an (absorbing) audience [15].

2.1.10   Early decay time

The early decay time, EDT, is another measure of the reverberation time in a room. Unlike T_{20} and T_{30} this quantity focuses on the early part of the impulse response, and uses the first 10 dB decrease of the sound pressure level, from 0 dB to -10 dB. When this value is multiplied by 6, the total 60 dB decrease is obtained. The reverberation time will often decrease more rapidly in this time window compared to the full impulse response, and this is the reason why the EDT is usually shorter than T_{30} and T_{20}.

The EDT is more important for subjective impressions and it is related to the perceived reverberation [13, p. 237], while T_{30} is more related to the physical reverberation [23]. The early decay time is more dependent on the early reflections in the room, and will thus be more dependent on the room geometry.

2.2 Geometrical variations

The reflected sound rays are important in concert halls and other rooms where there is a considerable distance from the sound source to the listener. The listener will receive reflections from the surfaces of the room, primarily the walls, the ceiling and a non-absorbing floor in addition to the direct sound. An uneven distribution of sound reflections will contribute to a room where acoustic quality differs between the listener positions.

Geometrical variations between rooms will influence on the distribution of sound reflections. The geometrical variations viewed in this thesis are based on polyhedral approximations of a dome with respectively six, nine and ten surfaces.

2.2.1 Wall inclination

In a trapezoid room, a case of the hexahedron shape, the reverberation time will be affected by the inclination angle θ of the walls. This effect is more significant for reflecting ceiling and walls. According to *Norges byggforskningsinstitutt* [12], the reverberation time can be doubled in the most extreme cases, and one will get maximal change in reverberation time when the walls are tilted approximately 5 ^{o} compared to the cuboid room. An angle $\theta > 90^o$ represents an outwards tilt, prolonging the reverberation time. If the walls are tilted inwards, $\theta < 90^o$, a shortening of the reverberation time can be expected.

The reason for the prolonged reverberation time with inclination angle $\theta > 90^o$ can be explained by following the ray paths. In this case, the rays will be reflected towards the reflecting ceiling to a higher degree, prolonging the reverberation time. When the walls are tilted inwards, a larger part of the sound will be reflected towards the floor which is the absorbing surface in the room for the situation of an absorbing audience. The reverberation time will then be shortened compared to the reverberation time of a shoe-box shaped room, and it may also be shorter than the predicted values by Sabine and Eyring.

2.2.2 Ceiling profile

U. Stephenson has been studying rooms of odd geometrical shape and the influence of the shape on the reverberation time. He states that the reverberation time is highly dependent on the room shape, especially in rooms where the absorption is unevenly distributed [24]. In the case of a concert hall, for instance, the total absorption is dependent on the size of the audience and will thus vary with the number of visitors.

In a paper from 2007 [25], Stephenson studied the dependency on the reverberation time by the longitudinal section of an auditorium and investigated whether it is possible to obtain reverberation times shorter than Sabine's prediction for certain ceiling profiles. It is known that the early decay time (EDT), together with the Deutlichkeit (D_{50}) and the decay of the sound pressure level are parameters that are dependent on the longitudinal section in general, and the ceiling profile in particular. Examples of concert halls with a 'tent shaped' ceiling profile are the *Philharmonie* in Berlin and the *Elbphilharmonie* in Hamburg. The latter is still in the state of construction.

The optimal volume per seat of a room is given by $V/N = 3 - 4$ m^3 for speech, $V/N = 6 - 12$ m^3 for music and $V/N = 5 - 8$ m^3 in mulitipurpose halls [12]. Beranek [10, p. 541] operates with an optimalization of $V/N = 9$ m^3 based on a selection concert halls, and a given reverberation time of $T = 2.0$ s.

The Elbphilharmonie is drafted for a number of 2150 in the audience, with a floor area of $A = 40 \cdot 60$ m^2 and a maxiumum height of $h = 30$ m. This height is the height in the middle of the room and the ceiling will have a tent shape, like a traditional circus. This makes the total volume $V > 30000$ m^3 giving an estimate of the volume per seat of $V/N \approx 15$ m^3 [25], which is above the recommended value of Beranek. Beranek's recommendation is, however, obtained in for instance the Philharmonie in Berlin.

In his examination of tent shaped halls, Stephenson found that the reverberation time decreased with the room angle. With specularly

reflecting walls, the reverberation time decreased by a factor of 1.5. For a higher diffusivity degree, the same effect could not be discovered.

2.2.3   Focusing effects

The shape of the ceiling surface is another factor that influences the sound distribution in a room, and consequently affects the reverberation time. Concave surfaces may have a focusing effect on the sound. For a curvature radius equal to the room height or twice the room height, these effects are most severe [12]. While a plane surface reflects specularly, a convex surface will disperse the sound and a concave surface, like a dome, will assemble the sound rays [26, p. 22]. If the concave surface has a focal point at the sound source or the sound receiver, the reflection may be heard as an echo.

By placing an acoustic absorber in the focal point of a concave surface, one may obtain a high efficiency of the absorber, making the effective absorption larger than the absorption coefficient given for the absorption material.

2.3   Predictions of the reverberation time

In acoustic computer models, geometrical acoustics is a common base for the simulations. Examples of geometrical acoustics are the two methods *image source method (ISM)* and *ray tracing (RT)*. There are benefits and disadvantages with both methods, and they are preferred for different applications. The two methods have in common that wavelength, or equivalent the frequency, is not a built-in characteristic [9, p. 235]. Therefore, the ISM and the RT often create higher order of reflections that one would obtain with wave theoretical acoustics.

A frequency dependent scattering coefficient of the surface is one way to implement the wave nature of the sound in geometrical acoustics. The implementation of the scattering coefficient in the simulations will be further described in section 3.2.2. The scattering coefficient will influence

the diffusivity of the sound field. A scattering coefficient of zero means that there are only specular reflections.

2.3.1 The Image Source Method

The image source method (ISM) is based on the boundary condition for a hard wall, where the particle velocity is zero, which makes it possible to replace the wall by a *mirror source*. A mirror source is an identical sound source as the main source, mirrored about the wall. The direct sound from the mirror source to the receiver will then be the exact specular reflection from the wall. [13, p. 102-109] For this to be valid, the reflections have to be purely specular, and it is not possible to implement a scattering coefficient in this method.
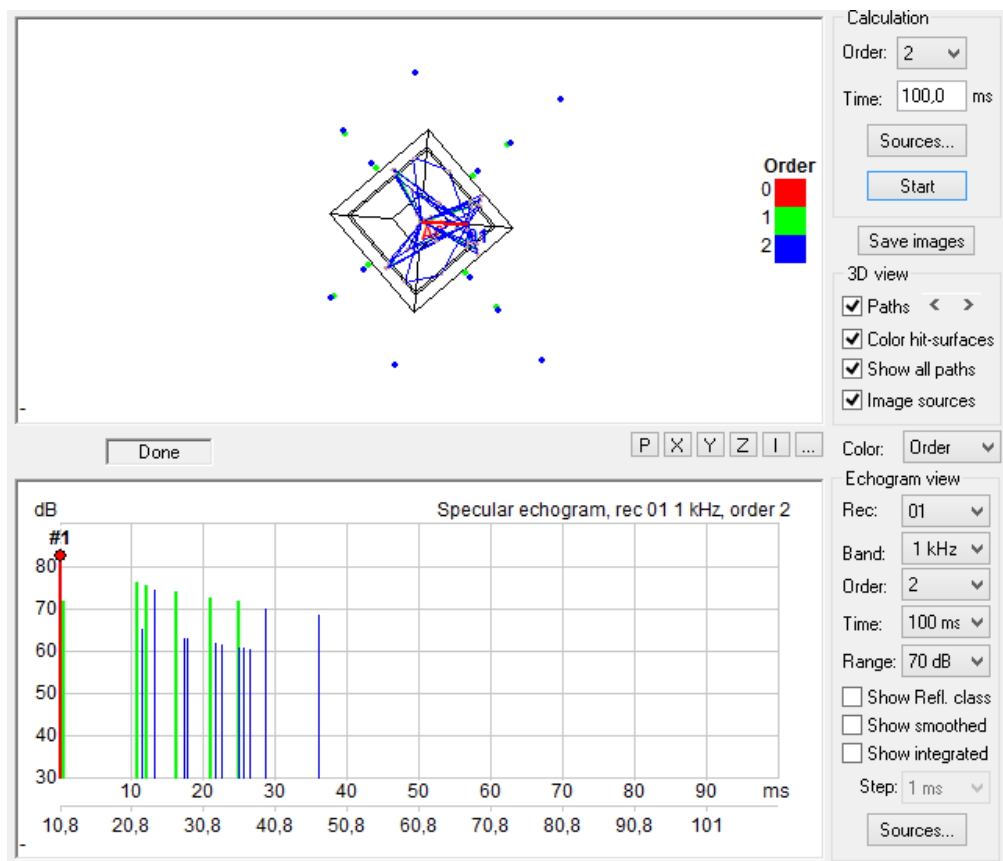
Figure 2.2: The image source method, illustrating the image sources (the blue and green dots) and the specular echogram.

The paragraph above explains how one concerns one specular reflection. To obtain a higher order of reflections, each mirror source is used as a new sound source and mirrored about the wall planes to obtain the total impulse response. This impulse response is then used to obtain parameters like the reverberation time. Figure 2.2 shows the implementation of the image source method, with the respective image sources, for 2nd order of reflections.

For a large number of reflections, use of the ISM is complicated and a prediction can take long time. The number of potential image sources grows exponentially with the number of reflections, but only a few are actually valid image sources. The ISM is therefore a good and accurate choice for simple, rectangular rooms where a low reflection order is sufficient. It is not preferred for complicated rooms where a high number of sound reflections is necessary to obtain a reliable result.

2.3.2   Ray Tracing and Cone Tracing

The 3-dimentional ray tracing method was first introduced at NTNU, Trondheim. Asbjørn Krokstad, Svein Strøm and Svein Sørsdal presented this method in 1968 [27]. The ray tracing method is still in use, based on the same principle as published in 1968.

In a ray tracing prediction one follows a large number of rays sent out from the sound source. Each time a ray hits a wall, it will be reflected either specularly, after Snell's law, $n_i sin(\theta_i) = n_r sin(\theta_r)$, or diffusely. A diffuse reflection will follow Lambert's law [28].

Whether the reflection is specular or diffuse is determined by the scattering coefficient s of the wall. The scattering coefficient is defined as the amount of energy which is not reflected specularly and has a value between 0 and 1. $s = 0$ means a pure specular reflection, while $s = 1$ gives a pure diffuse reflection. For a scattering coefficient between the two integers, the coefficient gives the probability of a diffuse reflection. Moreover, it follows that ray tracing is a stochastic method.

In a ray tracing the rays are followed for each reflection until they hit the

receiver. Then the impulse response is generated based on the total path length of each ray and the amount of absorbed sound. The cone tracing method is another version of ray tracing, where each ray is considered as a circular area, growing with time, substituting the rays with cones.

2.4 CATT-Acoustic

The prediction methods described in section 2.3 are examples of geometrical acoustics, and form a foundation for acoustical computer simulations. There exist different computer models, and the CATT-Acoustic calculation program is one of the computer models used in acoustics. CATT is an abbreviation for *Computer Aided Theatre Technique.* The newest version is CATT-Acoustic v9, which was released in 2011 [29].
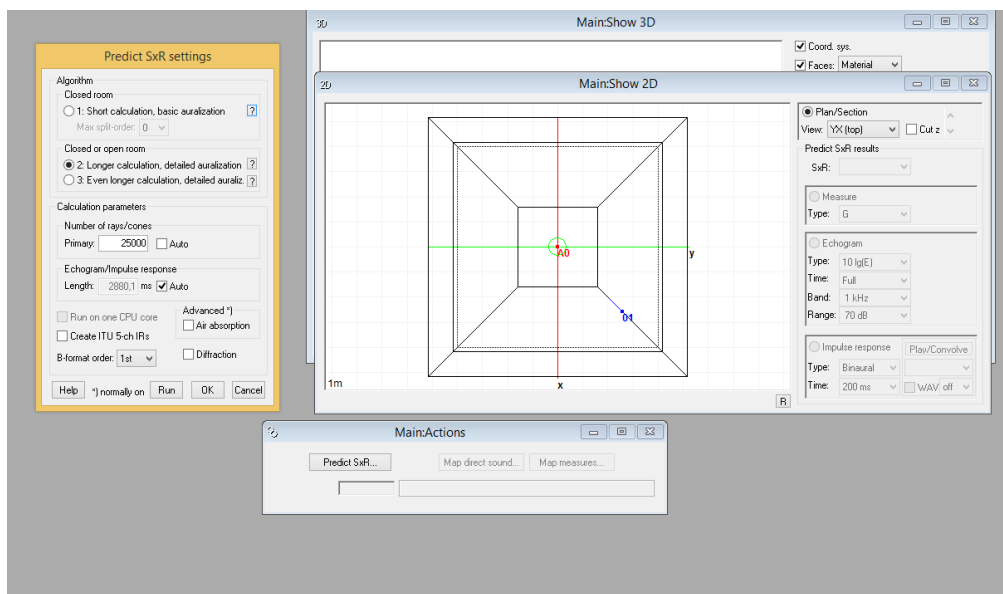
Figure 2.3: The CATT-Acoustic interface.

The CATT-Acoustic program contains two tools used to predict room acoustucal parameters: the *Interactive RT Estimate* and *TUCT - The Universal Cone Tracer.* Of these, TUCT is the main prediction and auralization program [30], and the interface of a TUCT prediction is

showed in Figure 2.3. The benefit of the Interactive RT-Estimate is that it indicates in which octave bands the assumptions of geometrical acoustics can be supposed to hold. This is also a prediction method that takes shorter time than the TUCT, so that one can use it to investigate the effect of diffuse reflections before performing a full TUCT.

2.4.1   The Universal Cone Tracer (TUCT)

TUCT modeling, which is a more detailed analysis than the Interactive RT Estimate, includes three different algorithms for cone tracing. These are based on the geometry of the room and the placing of sources and receivers. TUCT gives an opportunity for auralization, audience area mapping and estimation of room acoustical parameters. In this thesis only the estimated reverberation time from the echogram together with the formulae of Sabine and Eyring are investigated.

The TUCT is based on three algorithms of different complexity for a sound-receiver echogram or impulse response prediction and auralization. Algorithm 1 is only used for short calculations while algorithm 2 and 3 are used for the final calculations. All algorithms concern the frequency dependency of diffusivity and absorption. They use a combination of the image source method and ray tracing. In the case of the ISM, maximum third order reflections are concerned.

The first algorithm is a shorter calculation that uses a randomized diffuse reflection. This algorithm can handle the case of scattering $s = 0$. The second and third algorithms are longer calculations, and the second algorithm will be used in this thesis. Catt defines this algorithm as a *More advanced prediction based on actual diffuse ray split up suitable for more difficult cases, uneven absorption, open or very dry rooms. Also gives a low random run to run variation at the expense of a longer calculation time* [31].

3   Method

Before the simulations of the polyhedral rooms in CATT-Acoustic were performed, the dependency on the number of cones in the TUCT prediction was investigated. This performance is explained in section 3.1. The experimental work then follows in section 3.2 where the settings in the prediction mode of CATT-Acoustic are explained. This chapter also describes the statistical analysis of the results.

3.1   Investigation of the TUCT mode

To investigate the dependency of the number of cones in the TUCT simulations, there were performed simulations for the same room with four different combinations of floor absorption and scattering, with a range of cones from $N = 1000$ to $N = 50000$. In the four simulations, the walls and ceiling were hard surfaces with an absorption coefficient $\alpha_{wall} = 2\%$, and an absorbing floor with $\alpha_{absorber} = 90\%$ for all octave bands. Figure 3.1 shows the room with the small floor absorber present. The room is shoe-box shaped and has a volume $V = 13.9024 \cdot 13.9024 \cdot 6.9512$ m$^3 \approx 1344$ m^3.

The four configurations are combinations of two different sizes of the floor absorber and two different scattering coefficients. The small absorber has a surface area of $S_{abs,1} = 4 \cdot 4$ m^2 while the bigger absorber measures $S_{abs,2} = 12 \cdot 12$ m^2. For these absorber configurations, simulations were performed for scattering coefficients $s_A = 10\%$ and $s_B = 50\%$.

The results from these measurements will give an indication on the

importance of the number of cones necessary for a truth worthy result with the TUCT estimation tool and whether a systematic variation within the same geometry was present.
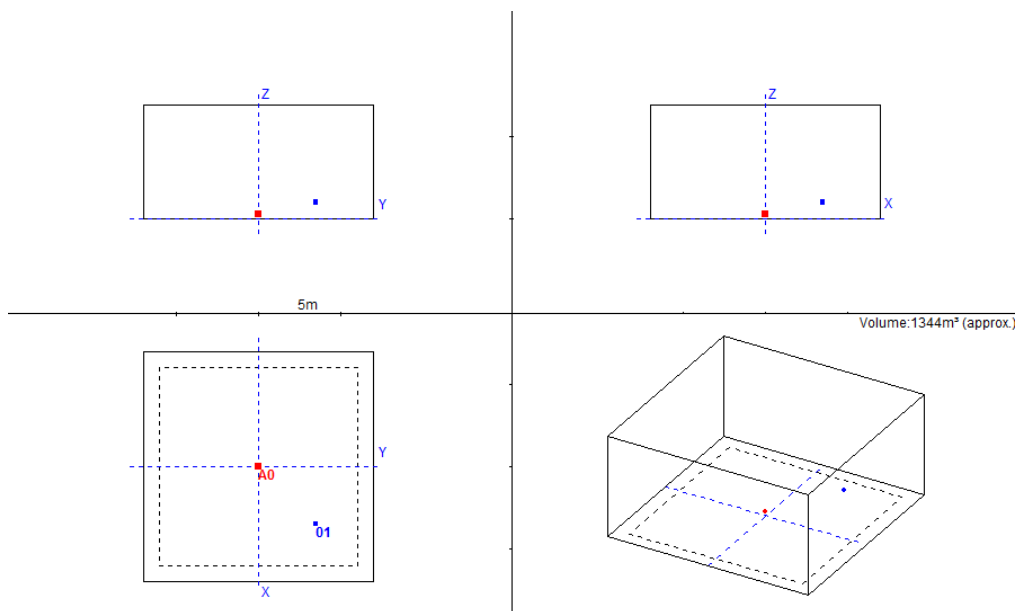
Figure 3.1: The room used to investigate the TUCT, here represented by the large absorber.

3.2 Simulations

3.2.1 Room geometries

In the search for rooms which give a shorter reverberation time than Sabine's and Eyring's formulae, polyhedral approximations of a dome were tested. To find the coordinates for the corners, the Matlab script added in appendix C.1 was run. This script gives, in cartesian coordinates, an output for the corners in a polygon approximation of a full circle, and by symmetry considerations the corner coordinates for the rooms implemented in CATT-Acoustic were found. The polygons correspond to a circle of radius 5 m with respectively 6, 8 and 10 corners; a hexagon, an octagon and a decagon, and the polyhedra were therefore approximations of a dome with this radius. To calculate the volumes and surface areas of the

polyhedra, the rooms were decomposed into simpler geometries and the formulae found in the Mathematical formulae-handbook [32, p. 32-37]. The corner coordinates can be found in Table 3.1.

Table 3.1: Corners of the polyhedra

Polyhedron	A (X, Y)	B (X, Y)	C (X, Y)	D (Z)	E (Z)
Hexahedron	5.4982	2.7491			4.7616
Nonahedron	5.2695	3.7621	0	3.7621	5.2695
Decahedron	5.1695	4.1822	1.5975	3.0386	4.9165

The X, Y, Z-coordinates are presented in Figure 3.2. The X- and Y-coordinates are equal due to symmetry. Figures 3.3, 3.4 and 3.5 shows the CATT files for these three geometries.
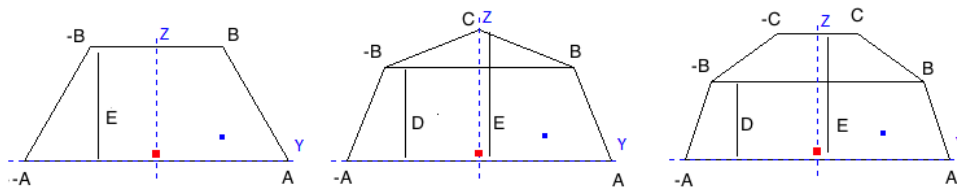
Figure 3.2: Coordinates of the three polyhedra.
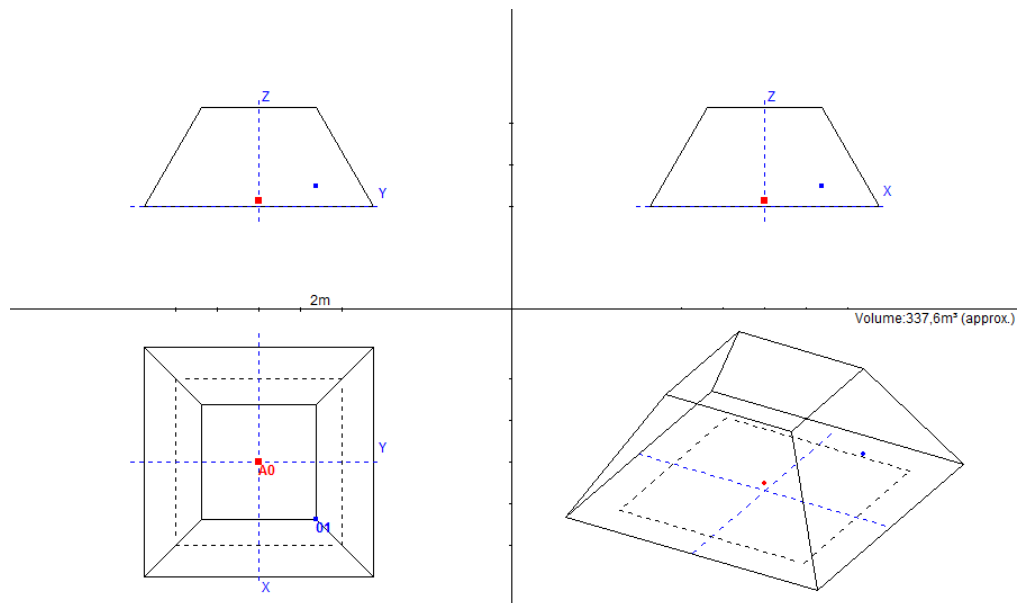
Figure 3.3: The hexahedron approach of a dome.
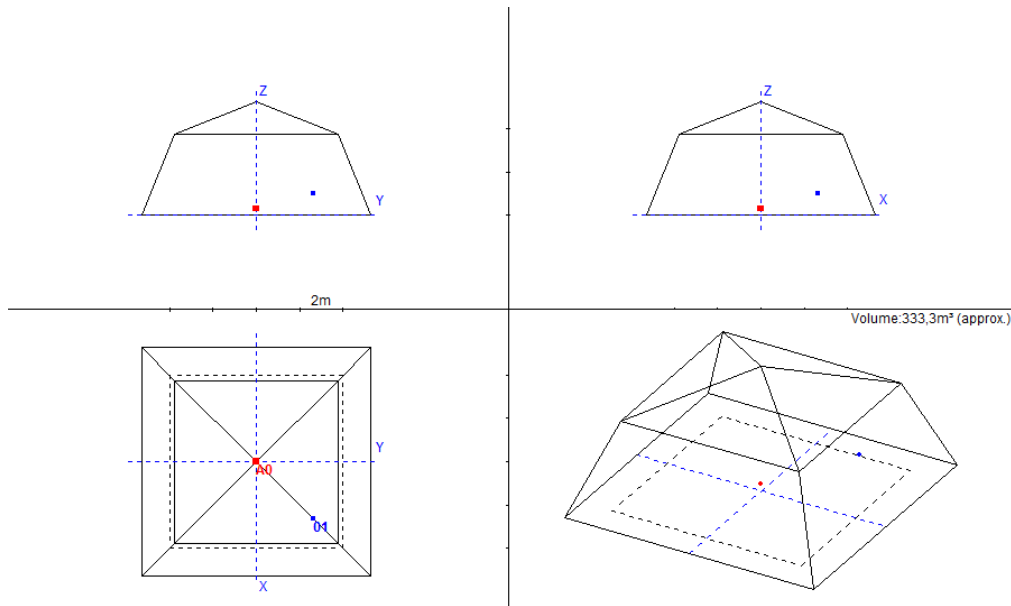
Figure 3.4: The nonahedron approach of a dome.
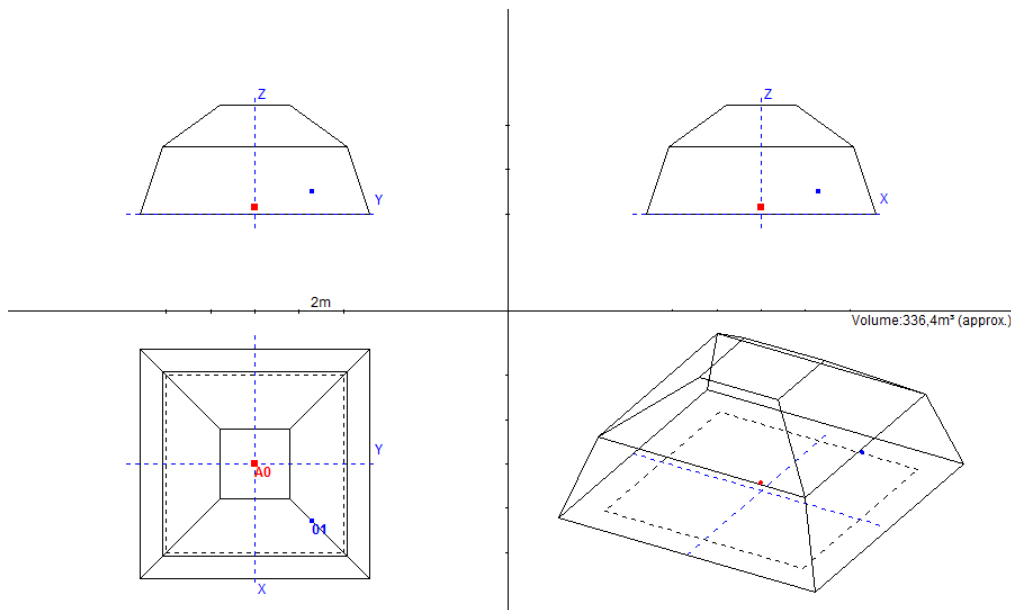
Figure 3.5: The decahedron approach of a dome.

For the hexahedron approach, there were also performed simulations for different wall inclination angles. The angles were varied for a room with constant volume and room height, given by the perfect dome approximation of inclination angle $\theta = 60^o$. With a constant room height, the surface area and average absorption did not vary significantly.

3.2.2   Settings in the prediction mode

In the prediction settings, air absorbtion was neglected, and the same accounts for the theoretical values where the air absorbtion term was not included. The influence of the air absorption is presented in section 2.1.7, and a consequence of neglecting the air absorption is that the simulated and predicted reverberation time will be higher than what one would measure in a real room.

Neglecting the air absorption, together with a choice of equal absorption- and scattering coefficients for all octave bands, give a selection of eight values corresponding to the octave bands from $f = 125$ Hz to $f = 16$ kHz. The values were used as a base for the statistical analysis, since the reverberation time is supposed to be independent of the frequency with the settings listed above.

The walls were chosen as hard walls, similar to those that were used in the scale model measurements carried out fall 2014. The absorption coefficient was therefore chosen as $\alpha_{hardwall} = 0.02$. The floor absorber was given an absorption coefficient of $\alpha_{absorber} = 0.90$. These values can be compared to *linoleum floor on concrete*, that varies from $\alpha = 0.02$ to $\alpha = 0.04$ for the different octave bands, and *perforated panel over isolation blanket, 10 % open area*, that varies from $\alpha = 0.85$ to $\alpha = 0.90$ for the octave bands in the range [250 Hz - 4 kHz]. A table of the absorbtion coefficient for the two materials can be found in appendix A.1 [20, p 341]. The size of this absorber varied between $S_1 = 4 \cdot 4$ m^2, $S_2 = 6 \cdot 6$ m^2 and $S_3 = 8 \cdot 8$ m^2.

In the CATT setup, there were used one omnidirectional sound source and one receiver. The source was placed in the center of the room, with a height of $h_{source} = 0.3$ m. The receiver was placed in $(X, Y) = (\frac{A}{2}, \frac{A}{2})$ with a height of $h_{receiver} = 1.0$ m.

3.2.3 Settings in the TUCT mode

Based on the investigation explained in section 3.1, a number of $n = 25000$ cones were chosen. The length of the impulse response was set to *auto*. CATT-Acoustic will then base the length of the impulse response on the Eyring value for the reverberation time. It is important to have a satisfying length of the impulse response to avoid a truncation effect where the resulting reverberation time becomes shorter than the true value.

The TUCT reverberation time estimations were done for scattering coefficients between $s = 1\%$ and $s = 90\%$ for the three polyhedra. The simulations then give a base for investigations of the relation between the size of the absorber, the number of surfaces, the scattering coefficient and the inclination angles of the hexahedron room. The relation will be presented in chapter 4.

3.3 Statistical approach

With settings kept independent of the frequency, the measured reverberation time will give a foundation of eight values for calculating the mean value and a 95%-confidence interval using the student-t-distribution [33, p. 261].

4 Simulation results

This chapter contains the results of the simulations performed in CATT-Acoustics. The figures are plotted as reverberation time (T_{30}, T_{Sabine} and T_{Eyring}) in seconds, as a function of the scattering coefficient. The simulated values from TUCT are represented by a 95%-confidence interval. The mean values can be found in appendix B. When the dependency on the size of the floor absorber, the inclination angle θ in the hexahedron approximation and the geometry are examined, the figures are plotted as $r = \frac{T_{30,TUCT}}{T_{Eyring}}$. A ratio $r < 1$ implies that the simulated result is shorter than Eyring's prediction of the reverberation time. For the dependency of the absorber, the ratio $\frac{T_{20}}{T_{30}}$ is also investigated for each polyhedron. The results of the investigation of the TUCT-mode in CATT-Acoustic are presented first, and the last section in this chapter contains a plot of the theoretical values for reverberation time.

4.1 Investigation of the TUCT mode

Figures 4.2, 4.3, 4.4 and 4.5 show the reverberation time T_{30} estimated with the CATT-Acoustic's TUCT-tool in a shoe-box shaped room shown in Figure 4.1, as a function of the number of rays used in the simulation.

The error bars in the figures indicate that the results of the simulations with the large absorber have a larger confidence interval than the simulations with the small floor absorber. Both the size of the confidence interval and the values of T_{30} appear to be independent of the number of rays. The TUCT estimate does vary within the same room, but this variation does

not follow the value of N. The random variation indicates an uncertainty of the simulations.

A low scattering coefficient, as shown in Figure 4.2 and 4.3, seems to give a greater variation of the T_{30}. The size of the absorber gives an indication of the relationship between the values of Sabine and Eyring and the estimated reverberation time, which follows the classical theory where one would assume the measured reverberation time to be longer than Sabine's and Eyring's formulae for an uneven absorption distribution and a low scattering, like the cases illustrated in Figure 4.2 and 4.3. For the scattering $s = 50\%$, the simulated and predicted reverberation times are almost identical.
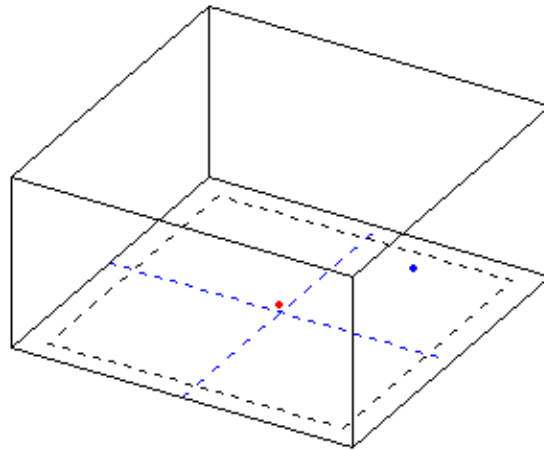
Figure 4.1: The room used for the simulations on the TUCT mode.
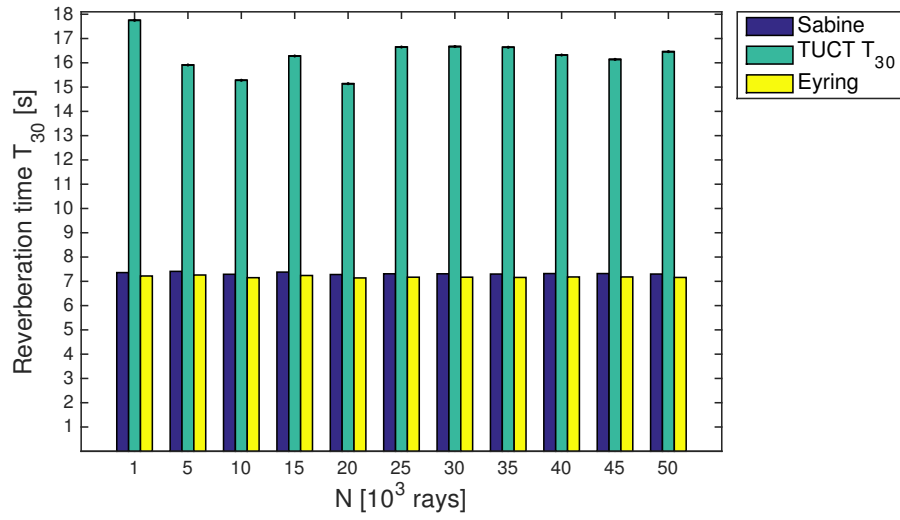
Figure 4.2: TUCT simulation in a shoe-box shaped room with 10% scattering and a small absorber.
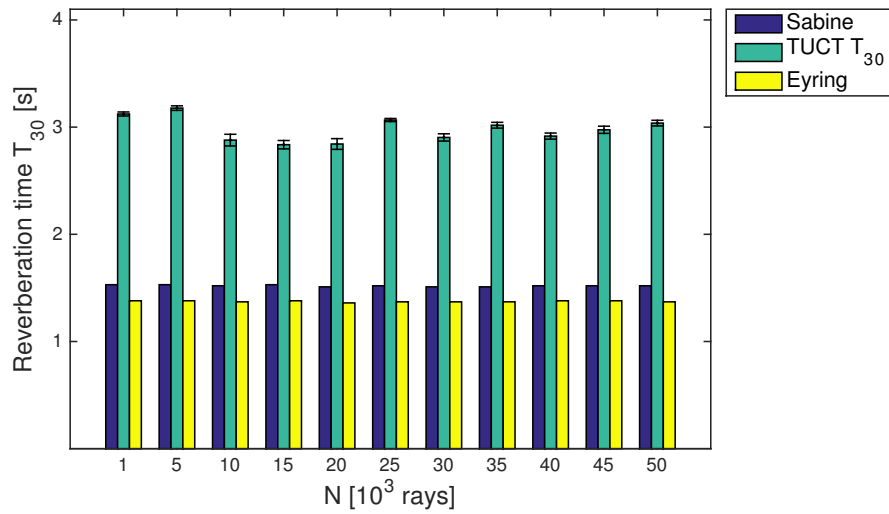
Figure 4.3: TUCT simulation in a shoe-box shaped room with 10% scattering and a large absorber.
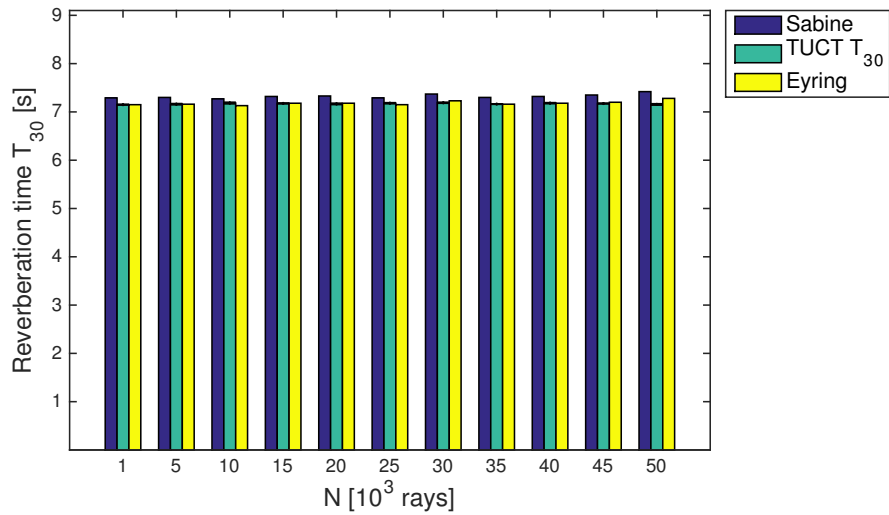
Figure 4.4: TUCT simulation in a shoe-box shaped room with 50% scattering and a small absorber.
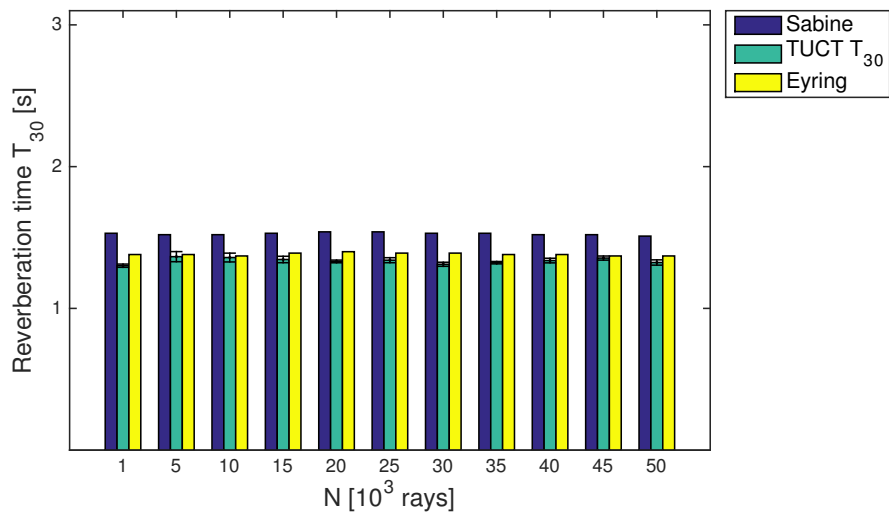
Figure 4.5: TUCT simulation in a shoe-box shaped room with 50% scattering and a large absorber.

4.2 Simulations in the hexahedron room

This section presents the results of the simulations of the hexahedron approximation to a sphere, the room showed in Figure 4.6. First, the variation in reverberation time as a function of the scattering coefficient is presented for a selection of inclination angles and the large floor absorber in the room. To show the dependency of the size of the absorber, a figure for the inclination angle $\theta = 60^o$ and scattering coefficients of $s = 10\%$, $s = 50\%$ and $s = 90\%$ with respect to the floor is shown in section 4.2.2. The dependency on the inclination angle then follows for the same scattering coefficients and absorber size.

Figure 4.6: The room used for the simulations in the hexahedron approximation.

4.2.1 Influence of the scattering coefficient

The relation between the simulated reverberation time $TUCT$ T_{30} and the estimations of Sabine and Eyring as a function of the scattering coefficient is plotted for seven inclination angles θ. There are some differences between these results which can be pointed out. For an angle $\theta = 60^o$, the simulated reverberation time is independent of the scattering coefficient. $\theta = 90^o$, the case of a cuboid room, gives a room with a pronounced dependency on the scattrering coefficient. Figure 4.8 shows a notable high value for the simulated reverberation time for $s = 1\%$.
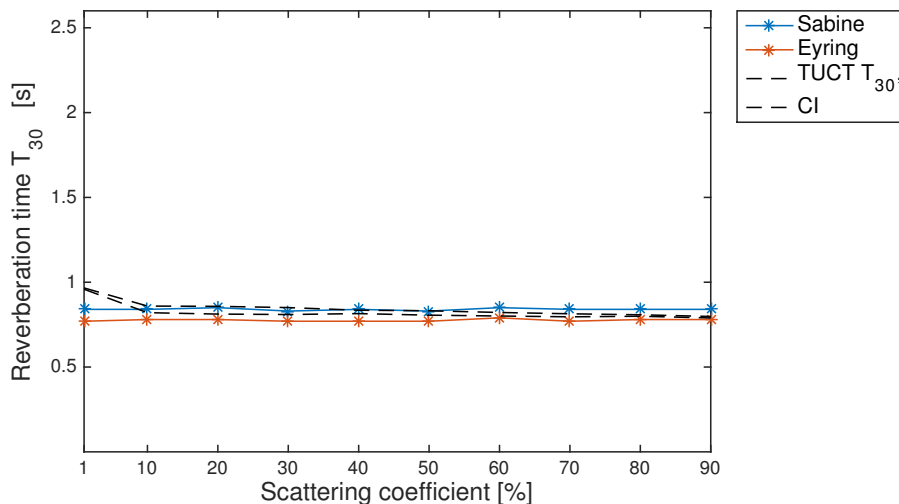
Figure 4.7: Reverberation time as a function of the scattering coefficient, hexahedron approximation and large absorber, angle $\theta = 35^o$.
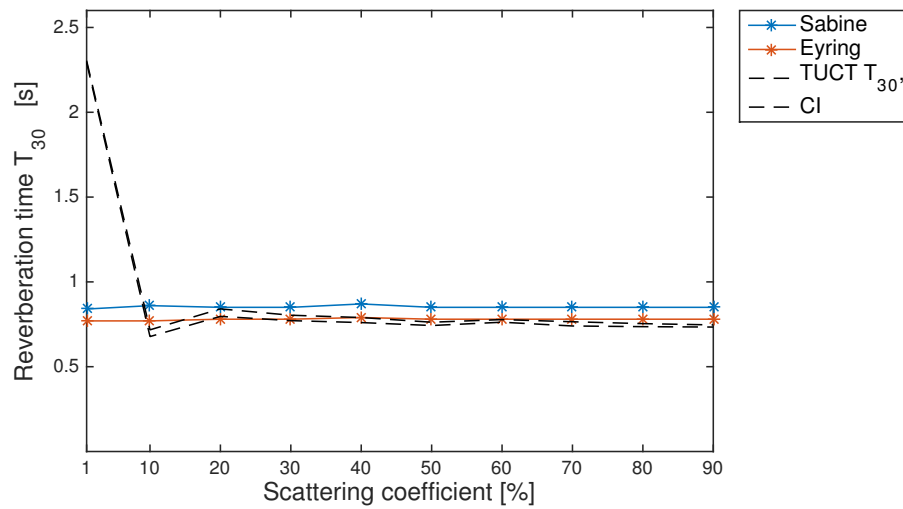
Figure 4.8: Reverberation time as a function of the scattering coefficient, hexahedron approximation and large absorber, angle $\theta = 45^o$.
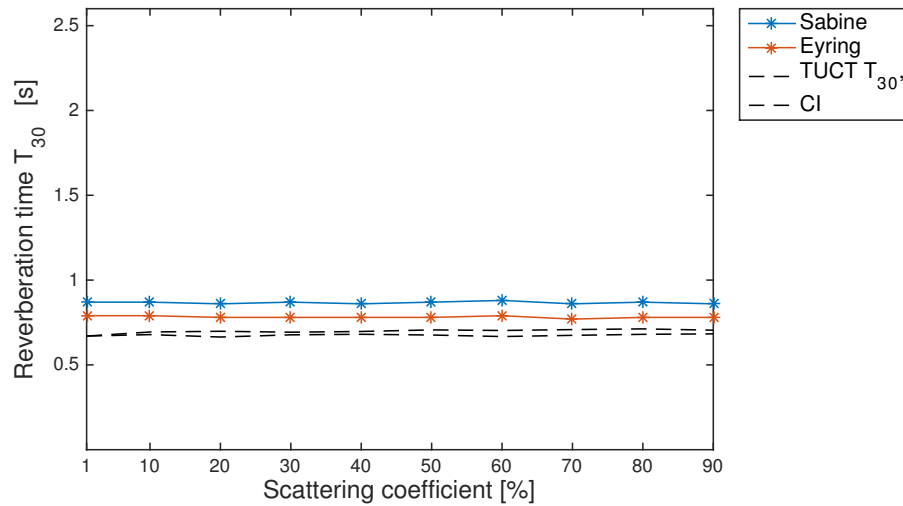
Figure 4.9: Reverberation time as a function of the scattering coefficient, hexahedron approximation and large absorber, angle $\theta = 60^o$.
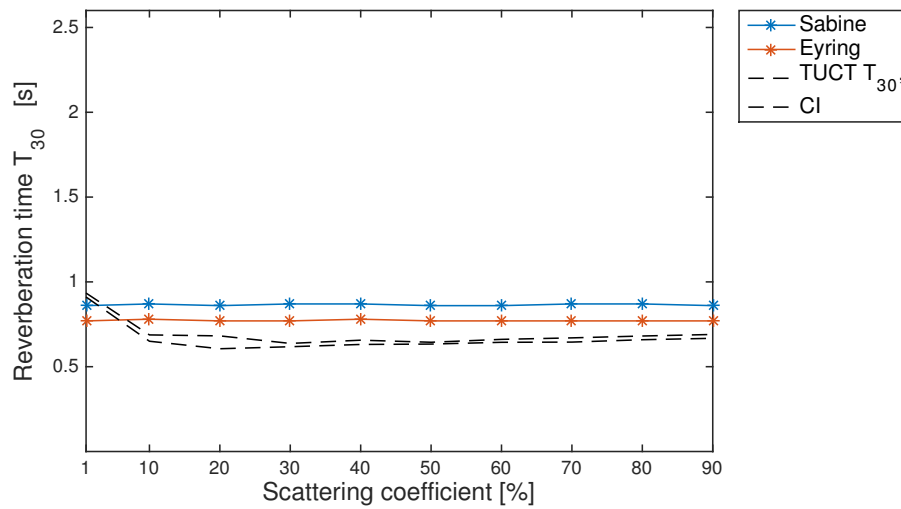
Figure 4.10: Reverberation time as a function of the scattering coefficient, hexahedron approximation and large absorber, angle $\theta = 75^o$.
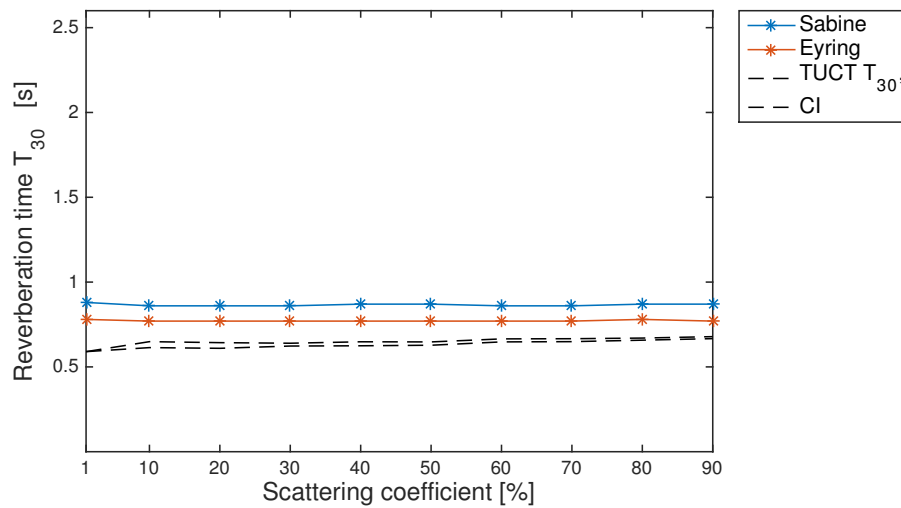
Figure 4.11: Reverberation time as a function of the scattering coefficient, hexahedron approximation and large absorber, angle $\theta = 82.5^o$.
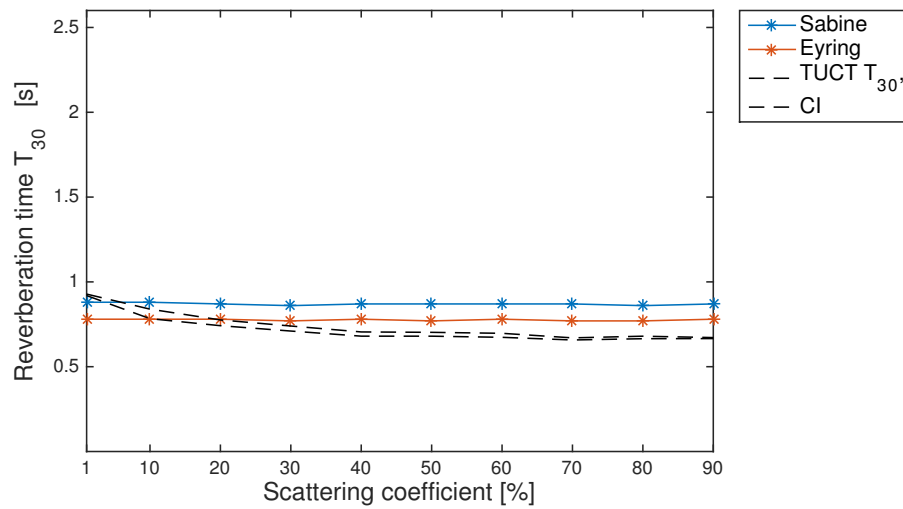
Figure 4.12: Reverberation time as a function of the scattering coefficient, hexahedron approximation and large absorber, angle $\theta = 87.5^o$.

Figure 4.13: Reverberation time as a function of the scattering coefficient, hexahedron approximation and large absorber, angle $\theta = 90^o$.

4.2.2 Influence of the size of the absorber

Figure 4.14 gives the relation between the size of the absorber and the reverberation time $r = \frac{T_{30}}{T_{Eyring}}$. A ratio $r < 1$ indicates that the mean value from TUCT is lower than the estimated value using Eyring's formula. Since Sabine's value is higher than Eyring's value for all situations, a ratio $r < 1$ implies that also the ratio $r = \frac{T_{30}}{T_{Sabine}} < 1$. Using the large absorber gives the lowest ratio.
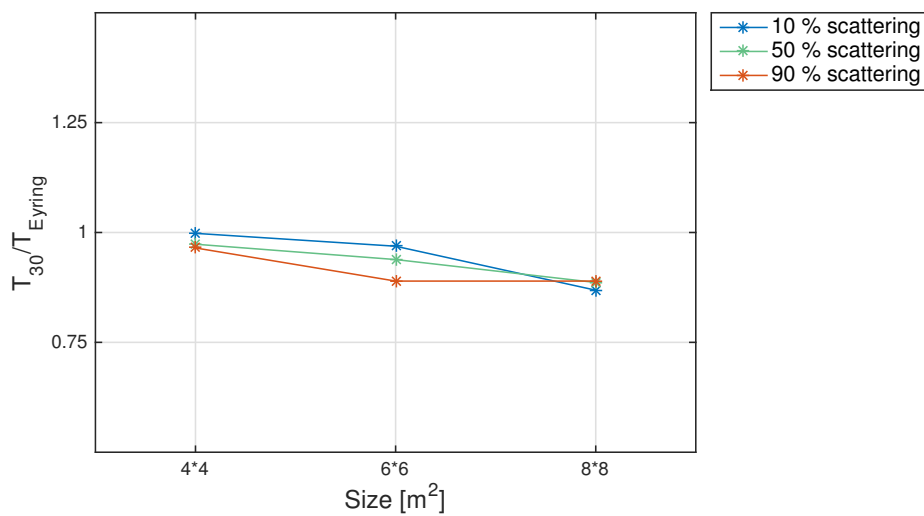
Figure 4.14: Reverberation as a function of the size of the absorber, hexahedron approximation and $\theta = 60^o$.

4.2.3 Influence of the inclination angle

The dependency on the inclination angle can be seen in Figure 4.15. In this figure, the room with the large absorber is considered. From this figure, one can see that the result of the shoe-box case ($\theta = 90^o$) is highly dependent on the scattering coefficient. For a higher scattering coefficient, it is not possible to discover the same extreme in the relationship of $\frac{T_{30}}{T_{Eyring}}$ and the geometry of the room.
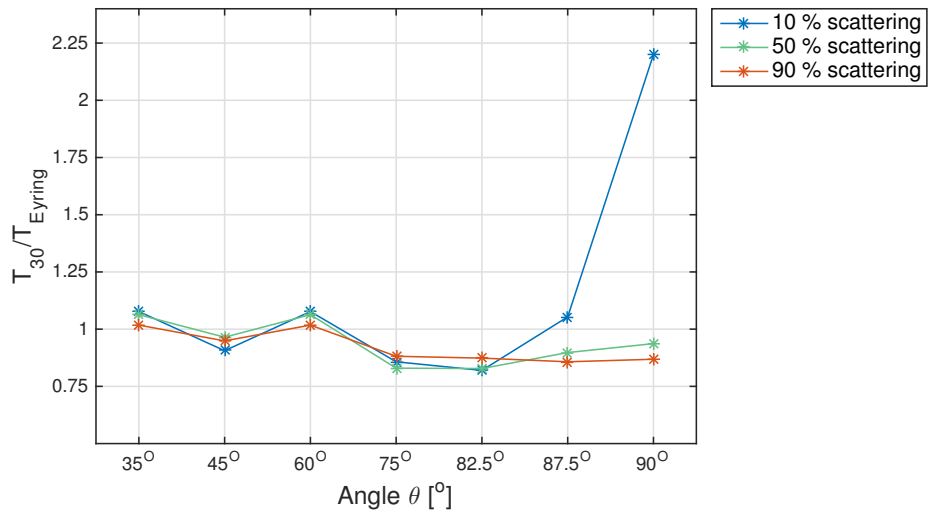
Figure 4.15: Reverberation as a function of the wall inclination angle θ, hexahedron approximation and large absorber.

4.3 Simulations in the nonahedron room

For the nonahedron approximation, illustrated in Figure 4.16, the wall inclination angle and the roof angle were kept constant. There were therefore two variables examined for this room; the scattering coefficient and the size of the absorber.
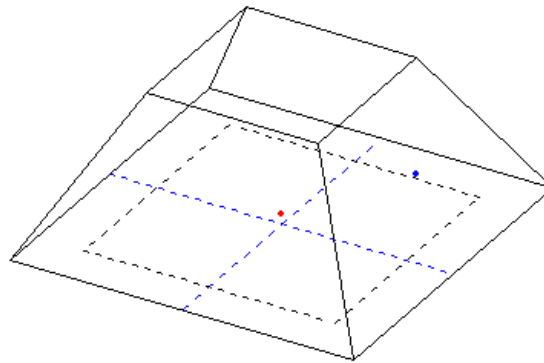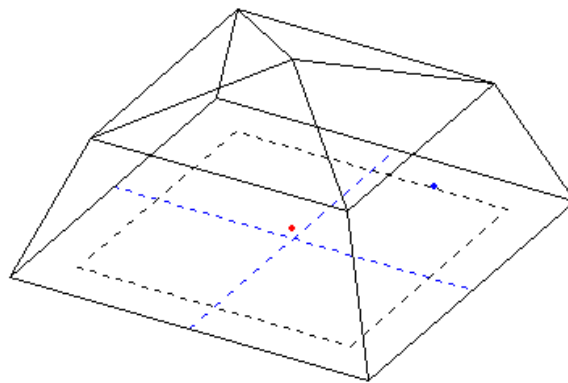

Figure 4.16: The room used for the simulations in the nonahedron approximation.

4.3.1 Influence of the scattering coefficient

From Figure 4.17 one can see that the scattering dependency on the reverberation time is most dominate for a low scattering coefficient. When the scattering increases ($s > 20\%$), the relationship between Sabine's and Eyring's values and the simulated reverberation time is nearly constant, with $T_{30} < T_{Eyring} < T_{Sabine}$.
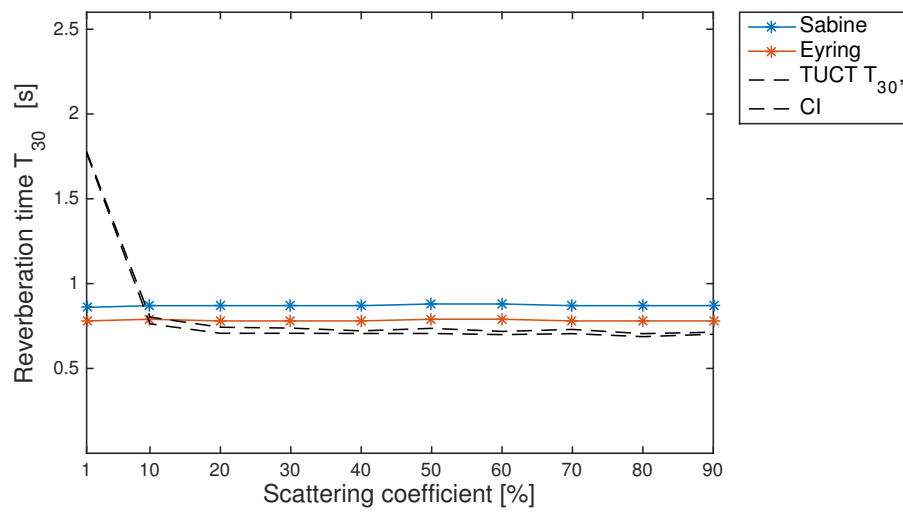
Figure 4.17: Reverberation time as a function of the scattering coefficient, nonahedron approximation and large absorber.

### 4.3.2 Influence of the size of the absorber

Figure 4.18 shows the same tendency as Figure 4.14, where a large absorber, or high scattering coefficient, is necessary to get a lower reverberation time than predicted by Eyring. For the absorber of size $8 \cdot 8$ m^2, the simulations for $s = 50\%$ and $s = 90\%$ are almost overlapping.
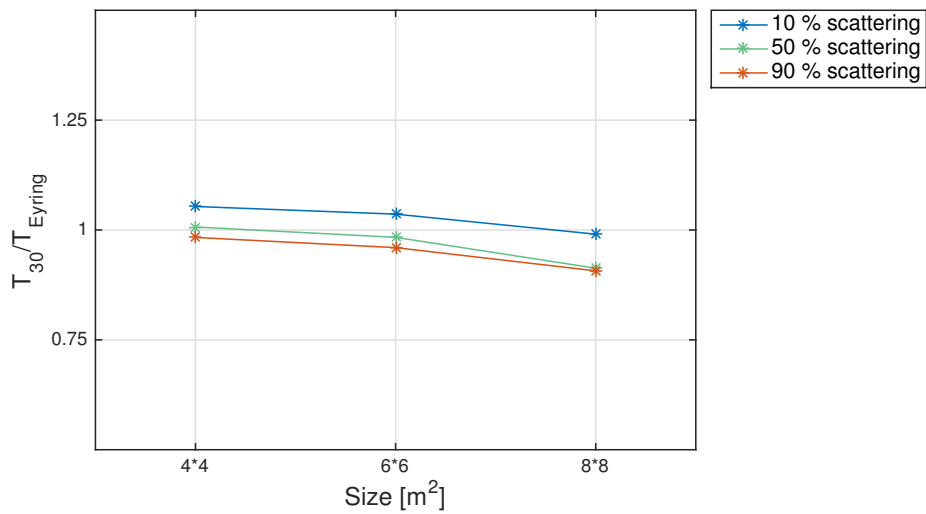
Figure 4.18: Reverberation time as a function of the size of the absorber, nonahedron approximation.

4.4 Simulations in the decahedron room

As for the nonahedron approximation, the inclination angles were kept constant for the decahedron room. This room is illustrated in Figure 4.19. The dependency on the scattering coefficient and the size of the absorber follows in section 4.4.1 and 4.4.2. As for the hexahedron and the nonahedron, the plot of the reverberation time as a function of the size of the absorber is given by $r = \frac{T_{30}}{T_{Eyring}}$.
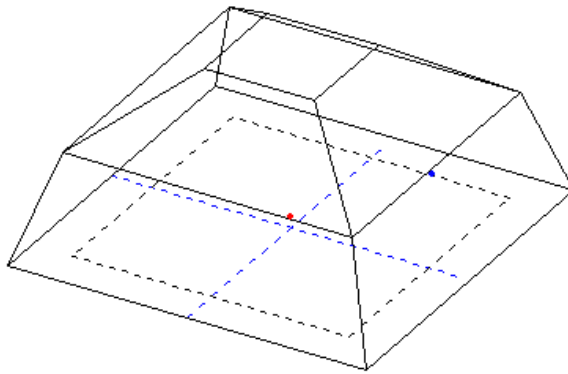
Figure 4.19: The room used for the simulations in the decahedron approximation.

4.4.1 Influence of the scattering coefficient

In Figure 4.20, the large floor absorber was used and the dependency on the scattering coefficent on the reverberation time is plotted. For a low scattering coefficient, $s < 20\%$, the simulated value overlaps with the estimation of Eyring. For a higher scattering coefficient, however, there is a significant decrease of the simulated reverberation time, compared to Sabine's and Eyring's values.
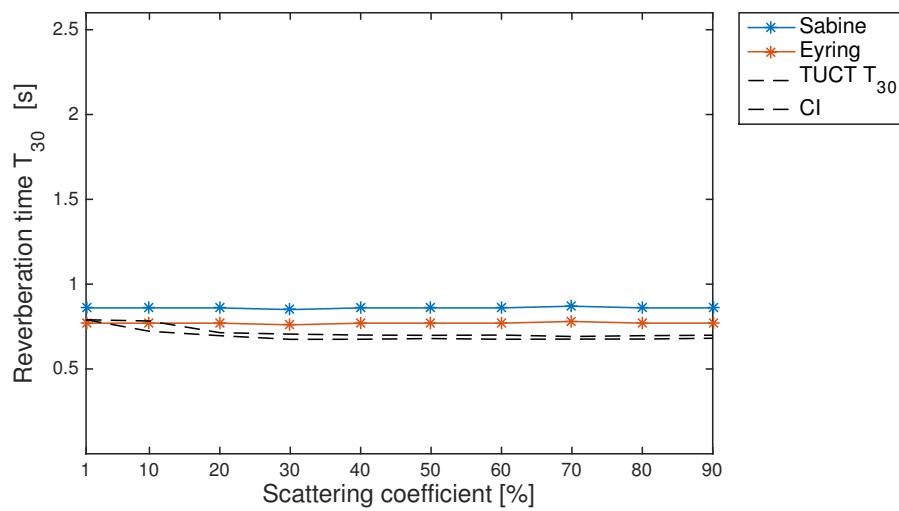
Figure 4.20: Reverberation time as a function of the scattering coefficient, decahedron approximation and large absorber.
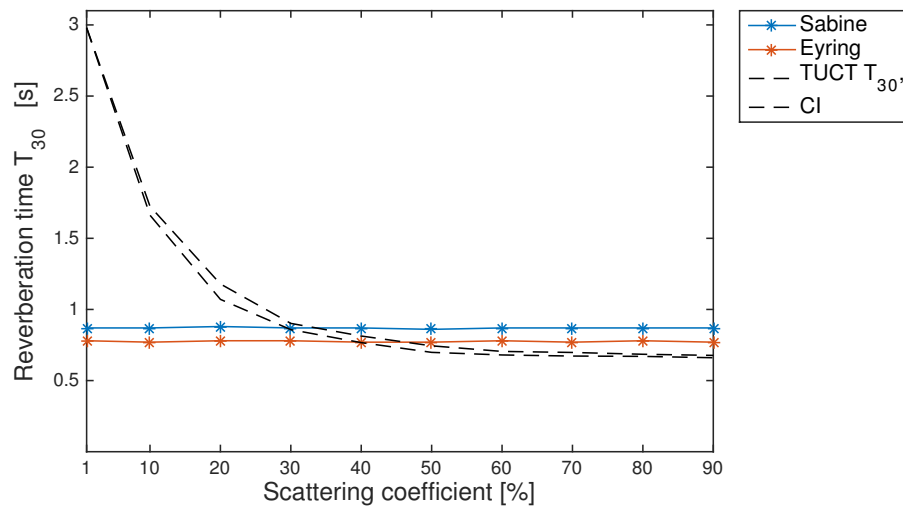
4.4.2 Influence of the size of the absorber

As one can see in Figure 4.21, a large absorber and a sufficient scattering coefficient is needed to generate a situation where the simulated reverberation time is shorter than Eyring's prediction. For $s = 10\%$, $r > 1$ for the small and medium absorber, and it is only slightly lower than one for the large absorber.
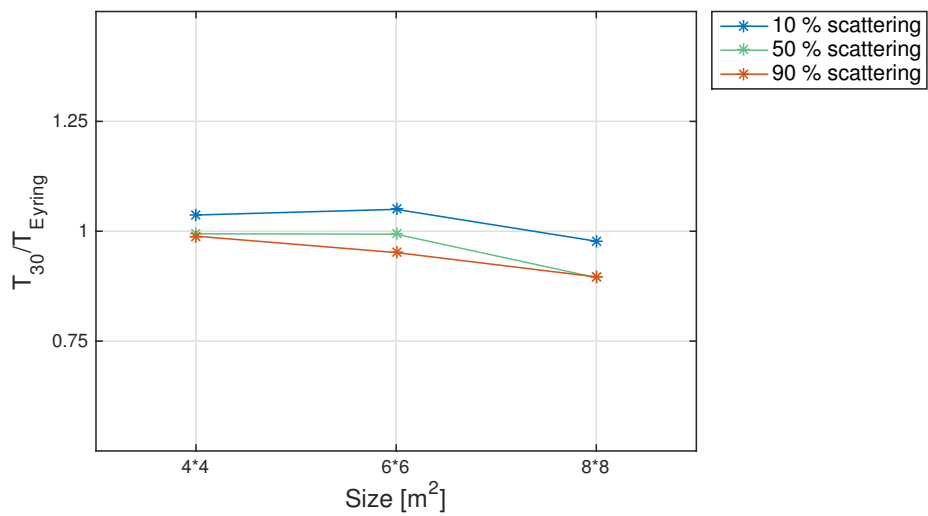
Figure 4.21: Reverberation time as a function of the size of the absorber, decahedron approximation.

4.5   Influence of the room geometry

To investigate the dependency on the number of surfaces in the polyhedra, Figure 4.22 illustrates the reverberation times in the three rooms for scattering coefficients of respectively $s = 10\%$, $s = 50\%$ and $s = 90$ %. The results follow from the simulations with the large absorber of $S = 8 \cdot 8$ m. From the figure, one can see that the relationship is nearly independent of the number of surfaces for a high scattering coefficient. The variation with geometry is more dominant for a low scattering coefficient.
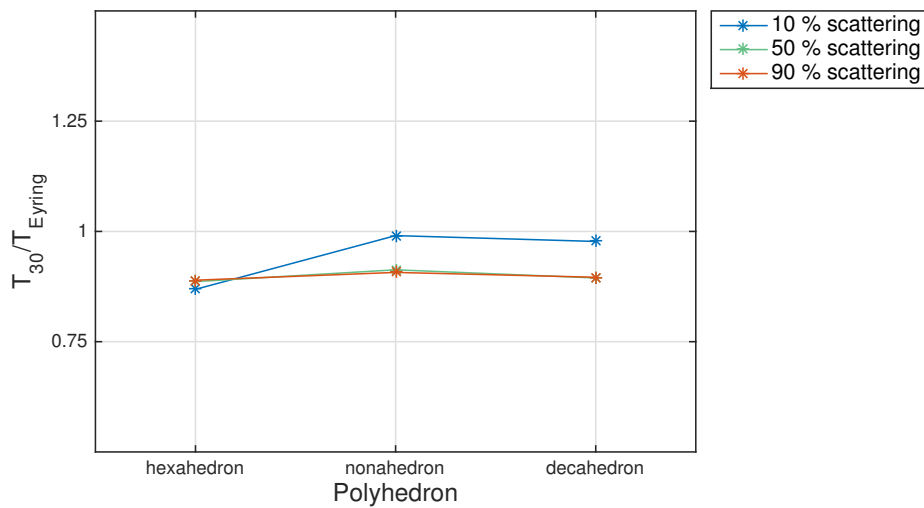
Figure 4.22: Reverberation time for the three polyhedral approximations, large absorber.

4.6   Alternative reverberation time formulae

In chapter 2, four different approaches to a theoretical value of the reverberation time were presented; Millington-Sette and Kuttruff in addition to Sabine's and Eyring's reverberation formulae. Reverberation times according to these formulae are presented in Figure 4.23, for the same room volumes and surface areas as the polyhedra which were simulated in CATT. The formula of Fitzroy, given in equation 2.25, is not included in this figure because it assumes a shoe-box shaped room, which is not the case in the rooms explored in this thesis. The theoretical values are presented together with the simulated values for a large absorber and respectively 10%, 50% and 90% scattering.
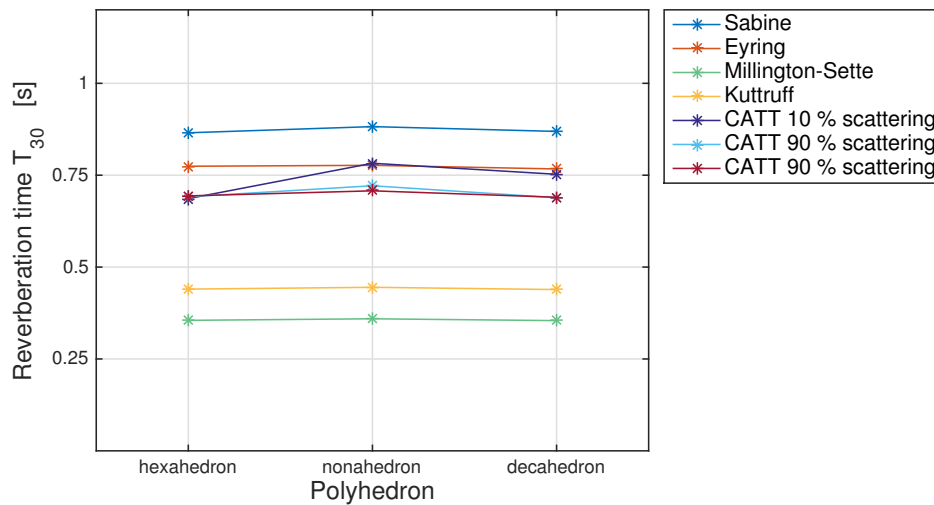
Figure 4.23:   Reverberation according to reverberation formulae, for different polyhedra, together with the simulated values from CATT.

4.7   Signs of a non-exponential decay

The relationship between the reverberation time based on respectively the first 20 dB decrease and the first 30 dB decrease indicates the linearity of the sound decay and thus the diffusivity of the sound field. This relationship $r = \frac{T_{20}}{T_{30}}$ was investigated for the three polyhedra, as a function of the size of the floor absorber, and is presented in Figures 4.24, 4.25 and 4.26.

In the hexahedron, the ratio $r \approx 1$, and the relationship appears to be linear for all sizes of the floor absorber and independent of the scattering coefficient. The results are more dependent on the scattering coefficient for the nonahedron and the decahedron, where the large absorber points out with the lowest ratio.
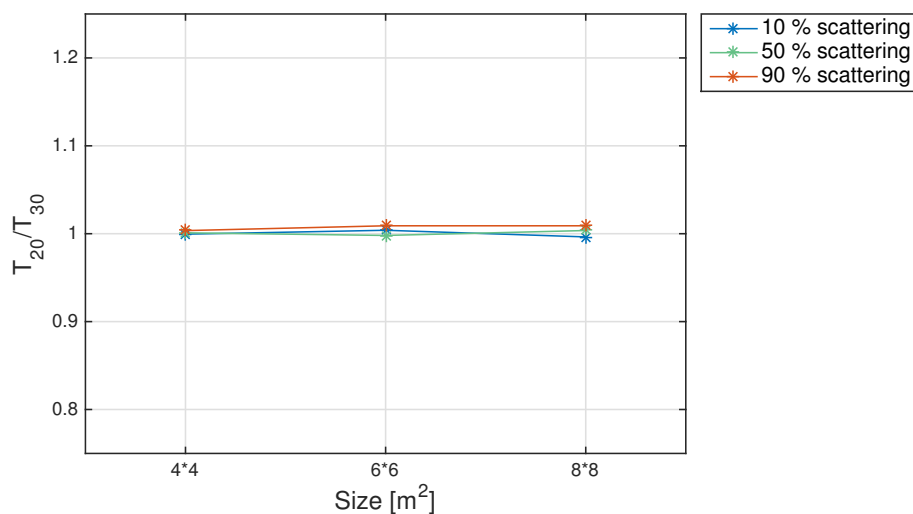
Figure 4.24: T_{20}/T_{30} for hexahedron, angle $\theta = 60^o$, as a function of the size of absorber.
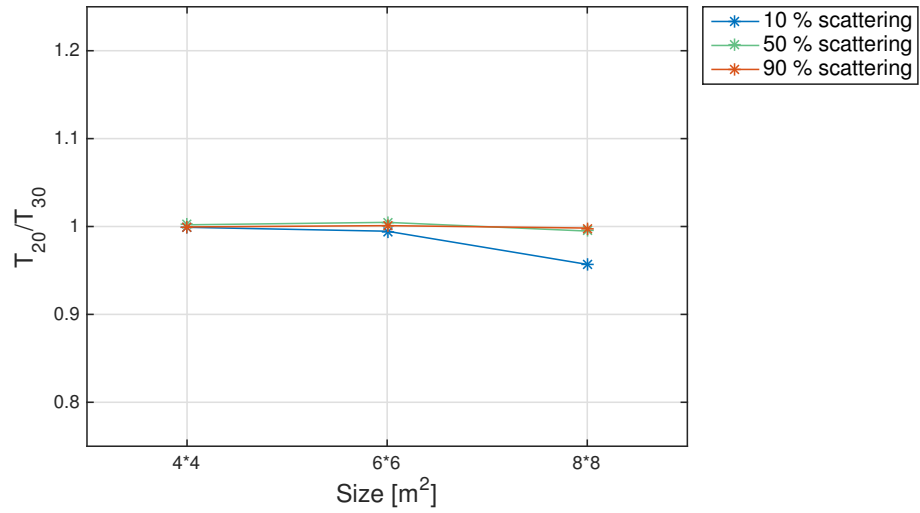
Figure 4.25: T_{20}/T_{30} for nonahedron as a function of the size of absorber.
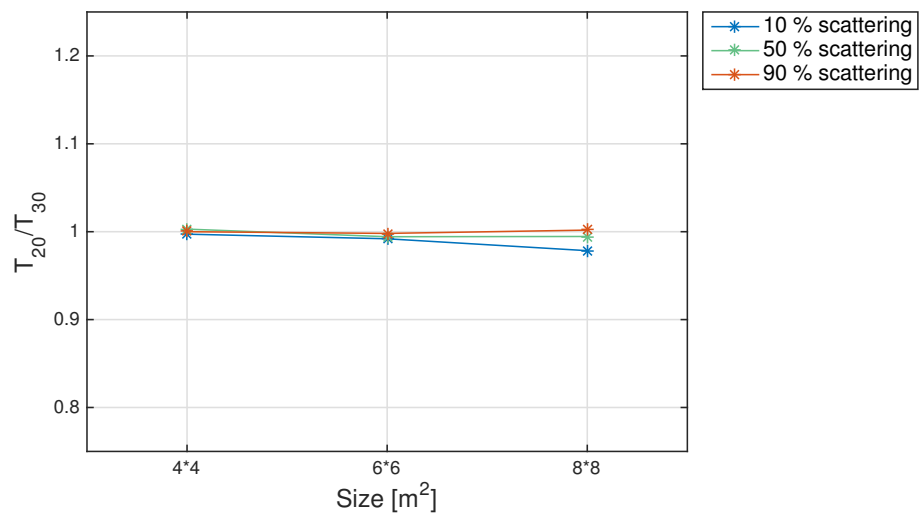
Figure 4.26: T_{20}/T_{30} for decahedron as a function of the size of absorber.

5   Discussion

Chapter 4 presented the results of the simulations in CATT-Acoustic, investigating the concequences of adjusting different parameters in the rooms. These results were also compared to theoretical values for the reverberation time. This chapter will discuss the results further. A discussion of the validity of the results will then follow, before a suggestion for further work is presented.

5.1   Investigation of the TUCT mode

The simulations in a shoe-box shaped room in TUCT described in section 3.1 were performed to investigate the importance of the number of cones necessary in a TUCT-estimate for different combinations of scattering and absorption. The two combinations with a high scattering coefficient gave rooms where the resulting reverberation time is known by Sabine's and Eyring's formulae.

The examination does not show a clear connection between the number of rays (N) in a simulation and the resulting reverberation time (T_{30}). The TUCT estimate does vary, but it is not a clear correlation to the number of cones. Figures 4.2 and 4.3 give an indication that a low scattering coefficient ($s = 10\%$) gives a higher variation between the simulations and thus a higher systematic error, while Figure 4.4 and 4.5 give more stable values of the T_{30}.

The combinations of scattering and absorption in the investigation of the TUCT mode also follow the theory regarding an increase in the scattering for a room with non-uniform absorption distribution and the measured reverberation time. While Sabine's and Eyring's values, based on the mean free path, show a little variation for one size of the floor absorber, the simulated values are highly dependent on the scattering coefficient.

5.2 Simulations in the hexahedron room

The scattering coefficient, the absorber size and the inclination angle were the three factors adjusted to investigate the resulting reverberation time in the hexahedron approximation. The correlation between these factors and the simulated reverberation time compared to the estimations of Sabine and Eyring will be discussed in this section. In the cases where the scattering coefficient and the inclination angle were adjusted, the large absorber was used. When the floor absorber and the inclination angle were varied, the chosen scattering coefficients were $s = 10\%$, $s = 50\%$ and $s = 90\%$.

5.2.1 Influence of the scattering coefficient

Figures 4.7, 4.8, 4.9, 4.10, 4.11, 4.12 and 4.13 in section 4.2.1 show the dependency on the scattering coefficient for inclination angles of respectively $\theta_1 = 35^o$, $\theta_e = 45^o$, $\theta_3 = 60^o$, $\theta_4 = 75^o$, $\theta_5 = 82.5^o$, $\theta_6 = 87.5^o$ and $\theta_7 = 90^o$. The result for $\theta_4 = 60^o$ shows an independency of the scattering coefficient that cannot be found from the other wall inclination angles. A possible explanation for this independency can be that the floor absorber has a higher efficiency when the angles of the polyhedron give a perfect approximation of a dome. This follows from the theory presented in section 2.2.3. However, as will be discussed in section 5.4, the number of surfaces in a polyhedra does not indicate that a focus effect can be the explanation.

For the smallest inclination angles. $\theta_1 = 35^o$ and $\theta_2 = 45^o$, a low scattering coeffient gives a significant longer reverberation time than predicted by Sabine and Eyring. This is a reasonable result, and one can see the same tendency also for larger inclination angles and scattering coefficient $s = 1\%$.

For an increasing scattering coefficient, the reverberation time appears to be less dependent on the inclination angle and the geometry. For θ_1 and θ_2, the simulated reverberation time approximates Eyring's and Sabine's values also for a high scattering coefficient. In the other simulations, however, the simulated reverberation time appears to be lower than the estimated values, as stated in the problem description.

5.2.2 Influence of the size of the absorber

The figure presented in section 4.2.2 shows an interrelationship between the size of the absorber and the ratio $r = \frac{T_{30}}{T_{Eyring}}$, which becomes lower relative to the size of the absorber. For the small absorber of $S_{abs} = 4 \cdot 4$ m^2, the estimated and simulated reverberation times are almost identical, giving a ratio $r \approx 1$ independent of the scattering. The same result applies for a low scattering coefficient and the medium-sized floor absorber. To lower the ratio of $\frac{T_{30}}{T_{Eyring}}$, one can see that it is necessary to apply a high scattering coefficient to the room with the medium absorber or to use the large floor absorber. A larger absorber, covering most of the floor, gives a result that is almost independent of the scattering coefficient.

In the latter case, a majority of the rays will hit the absorber, and thus shorten the sound decay in the room to a greater extent than the formulae of Sabine and Eyring predict. The opposite happens for the small absorber, especially for smaller angles θ resulting in a large floor area compared to the ceiling area, where a majority of the rays hit the floor outside of the absorber. A consequence is that a larger part of the rays is reflected, either specularly or diffusely, which prolongs the sound decay.

5.2.3 Influence of the inclination angle

From Figure 4.15, one can see that the angle between floor and walls in the hexagon approximation has an influence on the reverberation time. The reverberation time following the formulae of Sabine and Eyring, as given in equations 2.7 and 2.17, does not vary significantly. The reason for this is that the volume is kept constant for all angles, and that the total absorption area only has a minor deviation. However, one can see some variations in the theoretical values as well. The reason for these variations is that CATT-Acoustic calculates the volume of a room based on the resulting mean free path from a simulation, which may vary, as will be discussed in section 5.6.3. Smaller angles give simulated values closer to the reverberation times predicted by Sabine and Eyring, with a ratio $r \approx 1$.

An interesting result is found for $\theta_7 = 90^o$, the cuboid room, and $s = 10\%$, where the simulated value exceeds the estimated value giving a ratio of $\frac{T_{30}}{T_{Eyring}} \gg 1$. This is the same result as can be found in in the TUCT-investigation, illustrated in section 4.1. For higher scattering coefficients, the simulated value lies cloes to Eyring's prediction.

Figure 4.15 also supports what was stated in section 5.2.1, that the reverberation time is more dependent on the geometry for a low scattering coefficient. One can find a significant peak for $\theta_2 = 45^o$ and $\theta_7 = 90^o$ (the shoe-box shape), where the results for the shoe-box identify as highly dependent on the scattering coefficient.

An inclination angle $\alpha_3 = 60^o$ gives the perfect approximation of a dome. From the results in section 4.2.3, one can see that the results also for this geometry are less dependent on the scattering coefficient and the size of the a bsorber, and give a ratio of $r = \frac{T_{30}}{T_{Eyring}} \approx 1$. The connection between this geometry and the other polyhedra will be discussed further in section 5.4.

5.3 Simulations in the nonahedron and the decahedron rooms

The simulations in the nonahedron and the decahedron room were done for a varying scattering coefficient and three different floor absorbers, with a scattering coefficient of the surfaces varying from $s = 1.0\%$ to $s = 90\%$. The discussion for the two rooms is presented together in this section because the results show the same tendency for both polyhedra and the same parameters were adjusted in the two rooms.

5.3.1 Influence of the scattering coefficient

With the exception of a scattering coefficient of $s = 1\%$, the simulations from the nonahedron room with an absorber of $8 \cdot 8$ m^2 follows the same pattern as the hexahedron approximation with angle $\theta = 60^o$, which is as expected for the dome approximation.

For a low scattering coefficient, the resulting reverberation time is higher than what the formulae predict, due to a lower diffusivity in the room. In this case, the cone tracing will give a higher amount of specular reflections, and a smaller potential area of where a reflected cone may hit the next surface.

The simulations in the decahedron room do not show the same extreme as the nonahedron for a scattering of 1%, where the result gives a reverberation time of approximately the same value as Eyring's reverberation formula. For higher scattering coefficients, the simulations in the nonahedron and the decahedron rooms are almost identical.

5.3.2 Influence of the size of the absorber

A certain size of the floor absorber is necessary to finding the relationship in which the simulated reverberation time is shorter than Eyring's estimate. For the small absorber, $S = 4 \cdot 4$ m^2, the results give $\frac{T_{30}}{T_{Eyring}} > 1$, which

implies a prolonged reverberation time, which is what have been stated for rooms of other geometries (for instance a shoe-box shape with uneven absorption distribution) earlier. One can see that a higher value of the scattering coefficient leads to a reverberation time that is less dependent on the size on the absorber. This follows from both Figure 4.18 and 4.21.

5.4   Influence of the room geometry

With a high scattering coefficient, the resulting ratio $\frac{T_{30}}{T_{Eyring}}$ is independent of the room geometry, and identical for the three polyhedra. With a scattering of 10%, the hexahedron stands out with a ratio $r < 1$ independent of the size of the floor absorber. Figures 4.14, 4.18 and 4.21 shows the same tendency for the effect of the floor absorber, where this effect is largest for a high scattering coefficient. The results of the hexahedron simulations, which has the same ratio of $r \approx 0.88$ with the large absorber for all scattering coefficients, differs from the nonahedron and the decahedron.

A decahedron is the polyhedral approximation which is closest to the dome shaped room. One could therefore assume a possible focus effect to be stronger in this room. However, this is not the case, and the three polyhedra gives approximately the same ratio when the scattering is high. This is why a focus effect due to a dome shaped ceiling cannot be claimed to be the reason of why Sabine's and Eyring's formulae predicts a longer reverberation time than the simulations.

5.5   Alternative reverberation time formulae

From Figure 4.23, one can see that the simulated results lie closer the the Eyring value than the estimations of Millington-Sette and Kuttruff. Sabine's and Eyring's values are based on an assumption of a diffuse sound

field, which is not the case for the polyhedral rooms with uneven absorption investigated in chapter 4.

The Millington-Sette's formula was introduced with the purpose to be valid for rooms of uneven absorption distribution. One would therefore assume this formula to give a better estimate for the rooms examined in this thesis. However, as the figure shows, Millington-Sette predicts a lower value than the simulations in CATT-Acoustic. Using the absorption consideration of Kuttruff, the estimate is closer to the one found using TUCT, but also this value has a significant deviation from the simulations in CATT-Acoustic. One would assume Kuttruff's value lie closer to the simulated values since the situations all have $T_{30} < T_{Eyring}$, which is the range for the reverberation time in which Kuttruff's absorption formula is stated to be valid.

The fact that both Millington-Sette and Kuttruff predict a reverberation time shorter than Eyring and Sabine is an indication that the room geometries that have been investigated have provoked the difference between the reverberation formulae.

By investigating the deviation in the relations between respectively Eyring, Kuttruff and Millington-Sette and the simulated T_{30} for different scattering coefficients, the validity of the different formulae can be stated. This deviation is presented in Table 5.1. From these numbers, one can read that Eyring's formula stands out as the best approach to the result from the simulations in CATT-Acoustic. The formula of Kuttruff and Millington-Sette both give larger deviations from the true value. They correct, as is the intention of the formulae, for the fact that the absorbtion is unevenly distributed and the reverberation time therefore has to be lower than Eyring's prediction. However, both formulae can be told to overcompensate for this effect.

Table 5.1: The deviation between simulated reverberation time and theoretical formulae $T_{30}/T_{Formula}$.

Polyhedron	Sabine	Eyring	Millington-Sette	Kuttruff
Scattering $s = 10\%$				
Hexahedron	0.7930	0.8863	1.9329	1.5596
Nonahedron	0.7988	0.8927	1.9470	1.5710
Decahedron	0.8016	0.8958	1.9538	1.5765
Scattering $s = 50\%$				
Hexahedron	0.8870	1.0072	2.1777	1.7585
Nonahedron	0.8176	0.9284	2.0074	1.6209
Decahedron	0.8019	0.9107	1.9690	1.5899
Scattering $s = 90\%$				
Hexahedron	0.8658	0.9811	2.1239	1.7148
Nonahedron	0.7924	0.8979	1.9438	1.5694
Decahedron	0.7939	0.8996	1.9475	1.5724

From this table, one can see that there is a large positive deviation for Millington-Sette's formula and also a noticeable deviation in Kuttruff's formulae. This indicates that the simulated reverberation time is in some cases more than double the theoretical estimate.

These values could be compared to values presented by Neubauer and Kang [34] for their cases of a shoe-box shaped room with an absorbing ceiling ($\alpha = 0.8$) and reflecting walls and floor ($\alpha = 0.05$). Neubauer and Kang use an average over the frequency bands of $f = 500$ Hz and $f = 1$ kHz, and compare values by the formulae of Sabine, Eyring, Millington-Sette, and also Fitzroy, Arau and Fitzroy-Kuttruff, to simulations with CATT-Acoustic and the radiosity model. In their predictions, two sound sources and one receiver are used and the rooms have a constant diffusion of 10%. In both rooms, the simulated reverberation time is higher than Sabine's and Eyring's predictions, which is the classical example stated in the problem description.

The interesting element is their study of theoretical reverberation. In the first room, measuring $10 \cdot 10 \cdot 8$ m^3, the ratio of $r_{Eyring} = \frac{T_{Eyring}}{T_{Millington-Sette}}$ equals $r = \frac{1.14}{0.69} = 1.65$. The ratio of $r_{Sabine} = \frac{T_{Sabine}}{T_{Millington-Sette}}$ in this room has a value of $r_{Sabine} = \frac{1.27}{0.69} = 1.84$. For the room measuring $10 \cdot 10 \cdot 3$ m^3, the ratios equals $r_{Eyring} = \frac{0.45}{0.28} = 1.61$ and $r_{Sabine} = \frac{0.53}{0.28} = 1.89$.

Even if these ratios are not as extreme as what one can find in Table 5.1, they give the same tendency of $T_{Millington-Sette} \ll T_{Eyring}$ when only one surface is absorbing. The value of Fitzroy-Kuttruff, using Kuttruff's absorbtion approach as presented in section 2.1.9 in combination with Fitzroy's reverberation formula, lies between Millington-Sette and Eyring, which is the same relation as Kuttruff's aborption values in combination with Eyring's formula in the study of this thesis.

5.6 Uncertainty and statistics

A source of error that have already been introduced is the length of the impulse response in the TUCT-prediction. If the IR is too short, there is a risk of a truncation error [29, p. 110], which will lead to a simulated reverberation time that is shorter than the true value. To avoid such a situation, the length was set to *auto*. The length is then based on Eyring's value for the reverberation time. In this study, this length should be acceptable since the rooms studied have the relationship $T_{30} < T_{Eyring}$.

Other sources of error to be discussed are the locations of the source and the receiver, the degree of an exponential decay and the computation of the volume, which is based on the mean free path.

5.6.1 Placing of the source and receiver

In scale model measurements or full scale measurements of the reverberation time in a room, the measurement setup of sound sources and receivers would follow the ISO standard for measurements of reverberation time in ordinary rooms [6] and include multiple locations and heights of the source and the receiver. In this project, however, only one position for the sound source and one position for the receiver were chosen. The reason for this choice is that the reverberation time is considered a global parameter, and therefore independent of the location. This has been confirmed in a separate study in CATT-Acoustic which will not be presented in this thesis. The mean values and the statistical considerations were based on the

values for the respective frequency bands, which are independent of the frequency as a consequence of the settings presented in section 3.2.

5.6.2 Signs of a non-exponential decay

In the characteristics of a global paramenter, it follows that the sound decay is a pure expontential decay, meaning that the reverberation curve, given in dB, follows a linear curve. This is valid in most rooms, but exceptions follow for instance in coupled rooms.

By studies of the relation between T_{20} and T_{30}, as presented in Figures 4.24, 4.25 and 4.26, it is claimed that the two values will be identical if one has a pure exponential sound decay. T_{30} is based on the decay from -5 dB to -35 dB, while T_{20} is based on the decay from -5 B to -25 dB. The reason for excluding the first 5 dB decay is that the first part of the sound decay is strongly related to the direct sound in a room rather than the reverberation.

From the figures in section 4.7, one can see that the ratio $T_{20}/T_{30} \approx 1$ in all polyhedra for the small and medium floor absorber. In the hexahedron, this relationship also applies for the large absorber, and indicates a pure exponential sound decay. The other polyhedra, and in particular the nonahedron, seems to have a weakness for the large absorber, giving a ratio og $T_{20}/T_{30} < 1$, which means that the sound decay is not perfectly linear.

5.6.3 The mean free path and volume considerations in CATT-Acoustic

In the calculations of the total volume in CATT-Acoustic, the mean free path is used as a foundation, following from equation 2.5. The mfp is related to the average number of reflections in a ray tracing procedure, which is not a constant value. The reason that the Sabine and Eyring values have a variation within the same room is that these values are dependent on the volume V, which is supposed to be constant. A study of the difference in

volume calculated in CATT-Acoustic, compared to the values calculated in Matlab, should therefore indicate the uncertainty of the Sabine and Eyring values.

Table 5.2: Room volumes and mean free path calculated in CATT-Acoustics and in Matlab

Polyhedron	V_{Matlab}	$V_{CATT,mean}$	$V_{CATT,CI}$
Hexahedron	335.8697	339.1010	(337.3592, 340.8428)
Nonahedron	338.1679	339.4230	(338.2173, 340.6287)
Decahedron	333.6389	333.9550	(332.7722, 335.1378)
Polyhedron	MFP_{Matlab}	$MFP_{CATT,mean}$	$MFP_{CATT,CI}$
Hexahedron	4.3587	4.0800	(4.0579, 4.1021)
Nonahedron	5.0160	4.2640	(4.2488, 4.2792)
Decahedron	4.8674	4.3020	(4.2870, 4.3170)

Table 5.2 gives the values of the volume for each polyhedron approximation calculated in Matlab, together with the mean value from the TUCT-simulations and the 95% confidence interval for these values. The mean values and confidence intervals are based on the ten simulations for scattering $s \; \epsilon \; [1, 90]\%$.

In Figure 4.23, the values of Sabine and Eyring are calculated in Matlab using the correct volume and surface area. These values do not vary significantly from the values for Sabine and Eyring in the TUCT-predictions, and the statistical error due to the uncertainty in the mean free path can be stated to be small.

5.7 General comments

As can be deduced from the results and the previous discussion, the reverberation time following from geometrical acoustics and theoretical values is dependent on factors like the room shape, the distribution of the absorption and the scattering coefficient. The results indicates that there

is a limit for the scattering coefficient around $s_{limit} = 20\%$, where $s < s_{limit}$ gives simulated reverberation times which are not significantly shorter than T_{Eyring}, and in some cases higher than Eyring's prediction. The case of $s > s_{limit}$ does, however, give a ratio of $\frac{T_{30}}{T_{Eyring}} < 1$. The hexahedron with nclination angle $\theta = 60^o$ is an exception, and shows an independency of the scattering coefficient. As stated earlier, the assumption is that a low scattering coefficient gives a higher dependency on the room geometry, but this does not seem to be the case for this study. A low scattering coefficient results in most cases in a higher reverberation time, but the value for a low scattering coefficient does not seem to be dependent on the polyhedral approximations.

The formulae of Sabine and Eyring both assume a diffuse sound field, and give the same value for a room of constant volume and average absorption, while simulations based on the image source method and ray tracing give a variation with the respective factors. The study shows that neither Sabine, Eyring, Millington-Sette or Kuttruff can predict the same value for reverberation time as the TUCT-simulations in CATT-Acoustic. While Sabine and Eyring predict a value of the reverberation time higher than what was obtained in the simulations performed with CATT-Acoustic, Millington-Sette and Kuttruff give lower values than the simulated. The study shows that the value of Eyring lies closest to the simulated reverberation time.

The findings of Millington-Sette and Kuttruff both predicting reverberation times shorter than the values found by the TUCT-predictions indicates that the polyhedral room geometries in this study have resulted in the situations where the difference between the classical formulae by Sabine and Eyring and the correcting formulae by Millington-Sette' and Kuttruff's absorption formulae arises. The reason for these differences lies in the approach to the absorption coefficient and the absorption distribution.

5.8 Further work

As a consequence of what have been obtained in this thesis, there are several topics suggested for further work. It could be interesting to implement as scale model rooms, the rooms on which has been investigated in CATT-Acoustic, to see if the same tendency with a measured reverberation time lower than what Sabine and Eyring predicts can be found by performing measurements in a scale model. A correction for air absorption must then be included.

From the simulations in CATT-Acoustic, one could also study other room acoustical parameters than the reverberation time and their behavior in a polyhedron room. When studying the local parameters, one has to use several positions for the source and receiver, because one cannot assume these parameters to be the same in all positions.

Only a couple of theoretical approaches to a reverberation time have been investigated in this study, and there exist other alternatives as well. An example of a formula to investigate is Arau's reverberation formula [35]. Stephenson and Drechsler also suggest an *Anisotropic Reverberation Model (ARM)* [2], [36] assuming an anisotropic sound field, which can be investigated for the polyhedral rooms. Finally, the approach of Tohyama [37], based on an almost 2-dimentional diffuse field theory, could as well be tested on the polyhedra.

6 Conclusion

In this Master's thesis, the relationship between estimated reverberation times using classical equations and simulated reverberation times using the computational program CATT-Acoustic has been studied. These simulations are based on a combination of the image source method and a cone tracing-procedure.

The rooms that have been investigated are polyhedral approximations of a dome. As suggested by Stephenson, a tendency of a focus effect could be the case for such rooms. This effect could not be found in this study. The rooms implemented in CATT-Acoustic all had hard surfaces of $\alpha_{wall} = 2\%$ and a floor absorber on parts of the floor of $\alpha_{floor} = 90\%$. The parameters varied for each polyhedron were the size of the floor absorber and the scattering coefficient s. In the hexahedron approximation, also the wall inclination angle was adjusted, from $\theta = 35^o$ to $\theta = 90^o$. For these combinations, studies of the reverberation time were performed.

The simulations gave reverberation times shorter than Sabine's and Eyring's predictions for the polyhedra. It is, however, not possible to come to a conclusion that the polyhedral dome-approximations give a focusing effect; by increasing the number of surfaces in the polyhedron, the ratio of $\frac{T_{30}}{T_{Eyring}}$ did not vary significantly.

A reason for the difference between T_{30} and T_{Eyring} can be a higher effectiveness of the floor absorber when the side walls are tilted and the room has a saddle roof. The sound rays in the polyhedral approximations of a dome will then to a greater extent be reflected towards the absorbing floor, compared to a shoe-box shaped room or a trapezoid room with an inclination angle $\theta > 90^o$.

CATT-Acoustic has two approaches to finding the reverberation time. There is one simpler ray tracing tool, the *interactive RT estimate* and one more advanced, *The Universal Cone Tracer*. The latter one was used in the work of this thesis. The investigations of the TUCT-mode show a tendency to a variation in the simulated reverberation time for a varying number of cones. These variations do not follow an increasing number of cones, but seems to be a random variation.

For the polyhedral rooms, the ratio of $\frac{T_{20}}{T_{30}}$ was calculated to investigating the degree of an exponential sound decay. If this ratio $r \approx 1$, the reverberation time is independent of the dynamic range of the impulse response. $r \approx 1$ in the hexahedron, for all three sizes of the floor absorber and for scattering coefficients of respectively $s = 10\%$, $s = 50\%$ and $s = 90\%$. In the study of the nonahedron and the decahedron, the ratio $r < 1$ for the large floor absorber and a low scattering coefficient of $s = 10\%$, and indicates a tendency of a non-exponential decay. However, the ratio becomes $r \approx 1$ for a higher scattering coefficient and by using the small and medium floor absorber.

The predicted values of Sabine's and Eyring's equations are based on the volume which is related to the mean free path. This value varies within the same room for consecutive simulations, and is a source of error. The exact volume of the hexahedron and the nonahedron calculated with Matlab does not overlap with the 95%-confidence interval for the simulations in CATT-Acoustics. The confidence interval for the volume of the decahedron does, however, contain the exact value. For all three polyhedra, the mean free path-calculations from Matlab give a higher value than the simulations. However, the formula implemented in Matlab assumes a diffuse sound field which cannot be claimed for the polyhedral rooms with an uneven distribution of absorption.

Sabine's reverberation formula takes into account the room volume and the average absorption, in addition to a constant which is dependent on sound speed and thus temperature. The distribution of absorption is ignored in this equation. As a consequence, Sabine's formula predicts a reverberation time $T \rightarrow \frac{0.161V}{S}$ for an absorption coefficient $\bar{\alpha} = 1$, which is counterintuitive. Eyring wanted to correct for this weakness in the

formula of Sabine, and the formula of Eyring is based on an logarithmic consideration of the absorption coefficient, which gives the expected value of $T \to 0$ for $\bar{\alpha} = 1$. These two formulae give approximately the same values for a low average absorption.

Due to weaknesses also in Eyring's formula, other approaches of a reverberation time formula have been suggested. Two examples are Millington-Sette's formula and Kuttruff's formula, which have both been applied on the polyhedral rooms in this study. Millington-Sette and Kuttruff predict a reverberation time significantly shorter than the simulations in CATT-Acoustic. The relation of $T_{Sabine} > T_{Eyring} > T_{30,TUCT} > T_{Kuttruff} > T_{Millington-Sette}$, indicates that the geometry of the rooms considered in this Master's thesis provoke the difference between how the formulae treat the absorption distribution in a room.

The reverberation times predicted by Millington-Sette and Kuttruff are both significantly shorter than the classical Sabine's and Eyring's values. Moreover, the computer simulations in CATT-Acoustic leads to a reverberation time which is closer to Eyring's prediction than to the alternative formulae. This implies that Millington-Sette and Kuttruff do not seem to give a better alternative for the reverberation time in this study. For cases like the polyhedral rooms with an uneven distribution of absorption, a prediction for the reverberation time should be based on a detailed ray tracing-procedure, like what have been performed in CATT-Acoustic.

Bibliography

[1] H. Arau-Puchades, "The Refurbishment of the Orchestra Rehearsal Room of the Great Theater of Liceu," *Journal of Building Acoustics*, vol. 19, no. 1, 2012.

[2] U. Stephensen, "Effects of scattering on the reverberation time - does the definition of an 'equivalent scattering area' make sense?," *Forum Acusticum*, 2014.

[3] J. Vennerød, "The Hard Case - Improving Room Acoustics in Cuboid Rooms by using Diffusors - A student project report on scale model measurements, NTNU, Trondheim," *Published on `akutek. info`*, 2013.

[4] M. Skålevik, "How much scattering is sufficient to soften the hard case?," *Forum Acusticum*, 2014.

[5] M. Skålevik, "Reverberation time - the mother of all room acoustical parameters," *BNAM, published on `akutek. info`*, 2010.

[6] International Organization of Standardization, *Acoustics – Measurement of room acoustic parameters – Part 2: Reverberation time in ordinary rooms*, 2008.

[7] Norsonic, "Reverberation time measurements." Online; accessed 15.05.2015, `http://www.norsonic.com/?module=Articles&action=Article.publicOpen&id=503`.

[8] M. R. Schroeder, "New method of measuring reverberation time," *Journal of the Acoustical Society of America*, vol. 37, pp. 409–412, 1965.

[9] Z. Maekawa, J. H. Rindel, and P. Lord, *Environmental and Architectural Acoustics.* Spon Press, Taylor and Francis Group, second ed., 2011.

[10] L. Beranek, *Concert Halls and Opera Houses: Music, Acoustics, and Architecture.* Springer-Verlag, second ed., 2010.

[11] T. D. Rossing, ed., *Springer Handbook of Acoustics.* Springer, second ed., 2007.

[12] Byggforsk, "527.300 del 1, sending 2," *Byggforskserien - Byggdetaljer*, 1998.

[13] H. Kuttruff, *Room Acoustics.* Spon Press, Taylor and Francis Group, fifth ed., 2009.

[14] M. Skålevik, "Diffusivity and its significance to effective seat absorption in concert halls," *Published on akutek. info* .

[15] R. O. Neubauer, "Prediction of reverberation time in rectangular rooms with non uniformly distributed absorption using a new formula," *Acustica 2000*, 2000.

[16] W. C. Sabine, *Collected Papers on Acoustics.* Harvard University Press, 1922.

[17] C. F. Eyring, "Reverberation time in "dead" rooms," *The Journal of the Acoustic Society of America*, vol. 1, pp. 217–241, 1929.

[18] G. Millington, "A modified formula for reverberation," *The Journal of the Acoustic Society of America*, vol. 4, pp. 69–82, 1932.

[19] W. J. Sette, "A new reverberation time formula," *The Journal of the Acoustic Society of America*, vol. 4, pp. 193–210, 1933.

[20] L. E. Kinsler, A. R. Frey, A. B. Coppens, and J. V. Sanders, *Fundamentals of Acoustics.* John Wiley & Sons Inc., fourth ed., 2000.

[21] D. Fitzroy, "Reverberation formula which seems to be more accurate with nonuniform distribution of absorption," *The Journal of the Acoustic Society of America*, vol. 31, no. 7, pp. 893–897, 1950.

[22] H. Kuttruff, *Room Acoustics*. Spon Press, Taylor and Francis Group, fourth ed., 2000.

[23] International Organization of Standardization, *Acoustics – Measurement of the reverberation time with reference to other acoustical parameters*, 1997.

[24] U. Stephensen and H. Winkler, "Nachhallzeit-regulierung von auditorien durch neigung der seitenwände," *Fraunhofter-Institut für Bauphysic*, 1991.

[25] U. Stephensen, "On the influence of the ceiling profile on the distribution of the room acoustical parameters and the reverberation time," *International Symposium on Room Acoustics*, 2007.

[26] M. Barron, *Auditorium Acoustics and Architectural Design*. E & FN Spon, first ed., 1993.

[27] A. Krokstad, S. Strøm, and S. Sørsdal, "Calculating the acoustical room response by the use of a ray tracing technique," *Journal of Sound and Vibration*, vol. 8, pp. 118–125, 1968.

[28] B. I. Dalenbäck, "Engineering principles and techniques in room acoustics prediction," *BNAM*, 2010.

[29] *CATT-Acoustic introduction manual*.

[30] *CATT-Acoustic TUCT manual*.

[31] *CATT-Acoustic v9: Computer simulation program.* 2011, `http://www.catt.se`.

[32] K. Rottmann, *Matematisk formelsamling*, vol. 10. Spektrum forlag, 2008.

[33] R. E. Walpole, R. H. Myers, S. L. Myers, and K. Ye, *Probability and Statistics for Engineers and Scientists*. Pearson Education International, eight ed., 2007.

[34] J. Kang and R. O. Neubauer, "Predicting reverberation time: Comparison between analytic formulae and computer simulation," *International Congresses on Acoustics*, 2001.

[35] H. Arau-Puchades, "An improved reverberation formula," *Acoustica - International Journal of Acoustics*, vol. 65, pp. 163–180, 1988.

[36] S. Drechsler and U. Stephenson, "A calculation model for anisotropic reverberation with specular and diffuse reflections," *DAGA - Darmstadt*, 2012.

[37] M. Tohyama and A. Suzuki, "Reverberation time in an almost-two-dimentional diffuse field," *Journal of Sound and Vibration*, vol. 111, pp. 391–398, 1986.

A Tables

A.1 Coordinates for the hexahedron

Table A.1 gives the coordinates for the hexahedron room given different inclination angles, for a constant volume and room height.

Table A.1: Corners of the polyhedra, given different inclination angles.

Angle Θ	A	B	C
35 ^{o}	7.1121	0.3124	4.7616
45 ^{o}	6.3487	1.5871	4.7616
60 ^{o}	5.4982	2.7491	4.7616
75 ^{o}	4.8210	3.5452	4.7616
82.5 ^{o}	4.5058	3.8819	4.7616
87.5 ^{o}	4.3028	4.0949	4.7616
90 ^{o}	4.1993	4.1993	4.7616

A.2 Absorption coefficients

Table A.2 [20, p. 341] gives the absorption coefficients for two materials, corresponding to the absorption coefficients used in the simulations in CATT-Acoustic.

Table A.2: Absorption coefficients.

Material	125 Hz	250 Hz	500 Hz	1 KHz	2 KHz	4 KHz
Linoleum floor on concrete	0.02	0.03	0.03	0.03	0.03	0.02
Perforated panel over isolation blanket, 10 % open area	0.20	0.90	0.90	0.90	0.85	0.85

B   Mean values

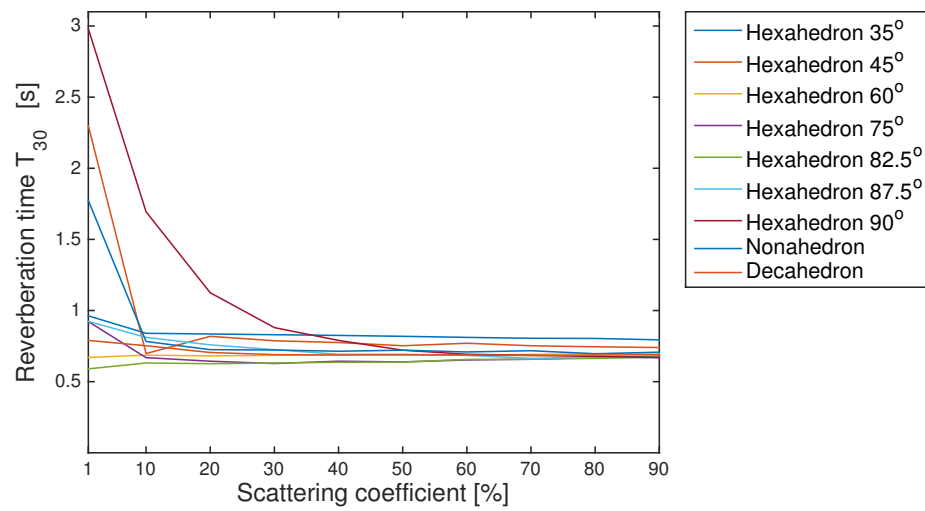Figure B.1: The mean values for the simulations of polyhedra with large floor absorber.

C Matlab code

C.1 Corners of a polygon

This scripts takes in the radius of a circle and the number of corners in the polygon approximation. By spherical symmetry, the coordinates are also valid for a polyhedron approximation of a sphere.

```matlab
%%%%%%%%%%%%%%%%%%%%%%%%%%
%% corners in a polygon %%
%%%%%%%%%%%%%%%%%%%%%%%%%%

% radius for the equivalent circle
r_c = 5;
% number of corners in the polygon approximation
numberofcorners = 6; % hexahedron

% radius of the polygon approximation
r_p = r_c*sqrt(2*pi/numberofcorners/sin(2*pi/numberofcorners));

% corners will contain the x- and y-coordinates of the polygon
corners = zeros(numberofcorners,2);
fivec = [0:numberofcorners-1].'*2*pi/numberofcorners;
% x-coordinates
corners(1:numberofcorners,1) = r_p*cos(fivec);
% y-coordinates
corners(1:numberofcorners,2) = r_p*sin(fivec);
```

C.2 Read out from .txt-file

In this script, a .txt-file from a TUCT-predition is read to find the reverberation times T_{Sabine}, T_{Eyring}, T_{30}, T_{20} and T_{15}.

```matlab
%%%%%%%%%%%%%%%%%%%%
%% read TUCT-file %%
%%%%%%%%%%%%%%%%%%%%

inputfile = 'TUCT_C3_3_10.txt'; % name of TUCT-file

% open TUCT-file
fid = fopen(inputfile,'r');
if fid == 0
    error(['ERROR: The file ',inputfile,' could not be opened.'])
end
B = fread(fid,inf,'char').';
fclose(fid);

% replace , by .
iv = find(B ==',');
B(iv) = '.';

stringtofind = '"s"';
iv_spaces = regexp(setstr(B),stringtofind);

stringtofind = '"RT''"';
iv_start = regexp(setstr(B),stringtofind);

% trim text from file
B = B(iv_start:iv_spaces(end));

% find lines that start with "(E)" and "s" in trimmed text file
stringtofind = '\(E\)';
iv_Epos = regexp(setstr(B),stringtofind);

stringtofind = '"s"';
iv_spos = regexp(setstr(B),stringtofind);

% find values for $T_{30}$, $T_{20}$ and $T_{15}$
```

```matlab
36  T15string = setstr(B(iv_Epos(3)+4:iv_spos(8)));
37  T20string = setstr(B(iv_Epos(4)+4:iv_spos(11)));
38  T30string = setstr(B(iv_Epos(5)+4:iv_spos(14)));
39
40  % one vector contains values for all eight octave bands.
41  iv_15 = find(T15string =='.');
42  T15values = zeros(1,8);
43  for ii = 1:8
44      T15values(ii) = str2num(T15string(iv_15(ii)-2:iv_15(ii)+2));
45  end
46
47  % one vector contains values for all eight octave bands.
48  iv_20 = find(T20string =='.');
49  T20values = zeros(1,8);
50  for ii = 1:8
51      T20values(ii) = str2num(T20string(iv_20(ii)-2:iv_20(ii)+2));
52  end
53
54  % one vector contains values for all eight octave bands.
55  iv_30 = find(T30string =='.');
56  T30values = zeros(1,8);
57  for ii = 1:8
58      T30values(ii) = str2num(T30string(iv_30(ii)-2:iv_30(ii)+2));
59  end
60
61  % Find values for Eyring and Sabine
62  stringtofind = 'Sabine';
63  iv_Sabine = regexp(setstr(B),stringtofind);
64  TSabinestring = setstr(B_A_1(iv_Sabine+7:iv_spos(16)));
65
66  stringtofind = 'Eyring';
67  iv_Eyring = regexp(setstr(B),stringtofind);
68  TEyringstring = setstr(B(iv_Eyring+7:iv_spos(17)));
69
70  % one vector contains values for all eight octave bands.
71  iv_Sabine = find(TSabinestring_A_1=='.');
72  Sabinevalues = zeros(1,8);
73  for ii = 1:length(iv)
74      Sabinevalues(ii) = str2num(TSabinestring(iv(ii)-2:iv(ii)+2));
75  end
76
77  % one vector contains values for all eight octave bands.
```

VIII

```matlab
78  iv_Eyring = find(TEyringstring =='.');
79  Eyringvalues = zeros(1,8);
80  for ii = 1:length(iv)
81      Eyringvalues(ii) = str2num(TEyringstring(iv(ii)-2:iv(ii)+2));
82  end
```